Flavor fluctuations in three-level quantum dots: Generic SU(3) Kondo fixed point in equilibrium and non-Kondo fixed points in nonequilibrium

Carsten J. Lindner,[1,2] Fabian B. Kugler,[3] Herbert Schoeller,[1,2,*] and Jan von Delft[3]
[1]*Institut für Theorie der Statistischen Physik, RWTH Aachen, 52056 Aachen, Germany*
[2]*JARA-Fundamentals of Future Information Technology, Aachen, Germany*
[3]*Physics Department, Arnold Sommerfeld Center for Theoretical Physics, and Center for NanoScience, Ludwigs-Maximilians-Universität München, Theresienstr. 37, 80333 Munich, Germany*

(Received 28 February 2018; published 29 June 2018)

We study a three-level quantum dot in the singly occupied cotunneling regime coupled via a generic tunneling matrix to several multichannel leads in equilibrium or nonequilibrium. Denoting the three possible states of the quantum dot by the quark flavors up (u), down (d), and strange (s), we derive an effective model where also each reservoir has three flavors labeled by u, d, and s with an effective density of states polarized with respect to an eight-dimensional F spin corresponding to the eight generators of SU(3). In *equilibrium* we perform a standard poor man's scaling analysis and show that tunneling via virtual intermediate states induces flavor fluctuations on the dot which become SU(3) symmetric at a characteristic and exponentially small low-energy scale T_K. Close to T_K the system is described by a single isotropic Kondo coupling $J > 0$ diverging at T_K. Using the numerical renormalization group, we study in detail the linear conductance and confirm the SU(3)-symmetric Kondo fixed point with universal conductance $G = 3\sin^2(\pi/3)\frac{e^2}{h} = 2.25\frac{e^2}{h}$ for various tunneling setups by tuning the level spacings on the dot. We also identify regions of the level positions where the SU(2) Kondo fixed point is obtained and find a rather complex dependence of the various Kondo temperatures as function of the gate voltage and the tunneling couplings. In contrast to the equilibrium case, we find in *nonequilibrium* that the fixed-point model is *not* SU(3) symmetric but characterized by rotated F spins for each reservoir with total vanishing sum. At large voltage we analyze the F-spin magnetization and the current in Fermi's golden rule as function of a longitudinal (h_z) and perpendicular ($h_\perp$) magnetic field for the isospin and the level spacing Δ to the strange quark. As a smoking gun to detect the nonequilibrium fixed point we find that the curve of zero F-spin magnetization in $(h_z, h_\perp, \Delta)$ space is a circle when projected onto the $(h_z, h_\perp)$ plane. We propose that our findings can be generalized to the case of quantum dots with an arbitrary number N of levels.

DOI: 10.1103/PhysRevB.97.235450

I. INTRODUCTION

Over the last three decades, transport properties of correlated quantum dots have gained an enormous interest in many experimental and theoretical research activities in condensed matter physics. As artificial atoms they allow for a controlled study of interesting phenomena playing a central role in many different fields of applied and fundamental research in nanoelectronics, spintronics, quantum information processing, dissipative quantum mechanics, and many-body physics and nonequilibrium phenomena in correlated systems (see, e.g., Refs. [1,2] for reviews). Of particular interest is the cotunneling or Coulomb blockade regime of quantum dots with strong charging energy, where the charge is fixed and only the spin and orbital degrees of freedom can fluctuate by second-order tunneling processes via virtual intermediate states. In this regime, effective models can be derived which are equivalent to Kondo models well known from solid-state physics [3] (see, e.g., Ref. [4] for a review of the Kondo effect in quantum dots). The standard model is the SU(2) Kondo model, where a local spin-$\frac{1}{2}$ is coupled via an isotropic exchange coupling to the spins of two large reservoirs. Below a characteristic low-energy scale, called the Kondo temperature T_K, the local spin is completely screened and the remaining potential scattering leads to resonant transport through the system with universal conductance $2\frac{e^2}{h}$. This Kondo effect has been theoretically predicted for quantum dots [5] and has been experimentally observed [6]. After this discovery, the research for Kondo physics in quantum dots has gained an enormous interest and further realizations have been proposed and observed, such as, e.g., the realization of higher spin values [7], singlet-triplet fluctuations [8], non-Fermi-liquid behavior in two-channel realizations [9], and the SU(4) Kondo effect [10]. Recently, also the realization of SU(N) Kondo physics for arbitrary N has been proposed in coupled quantum dots [11–13].

The enormous variety of possible realizations of Kondo physics raises the question as to what happens in the generic case when a quantum dot in the regime of fixed charge with $N_{\rm dot} \geqslant 1$ electrons and $N \geqslant 2$ levels is coupled via a generic tunneling matrix to several multichannel reservoirs. Even for the simplest case $N_{\rm dot} = 1$ and $N = 2$, this issue is nontrivial since the quantum number $l = 1,2$ labeling the two dot levels is in general a nonconserved quantity in tunneling, such as, e.g., for ferromagnetic leads [14], orbital degrees of freedom

*schoeller@physik.rwth-aachen.de

[15], Aharonov-Bohm geometries [16], and spin-orbit or Dzyaloshinski-Moriya interactions [17,18]. In Ref. [16] it was shown via a singular value decomposition of the total tunneling matrix (i.e., containing *all* reservoirs) that all these different cases can be mapped onto an effective model which is equivalent to the anisotropic spin-$\frac{1}{2}$ Kondo model which flows into the isotropic SU(2)-symmetric fixed point at low energies below the Kondo temperature. This explains why in all linear response transport calculations of quantum dot models with $N_{\rm dot} = 1$ and $N = 2$, the Kondo effect with universal conductance is observed provided that local effective magnetic fields are explicitly canceled by external ones [19]. However, this result is only valid in the linear response regime and for proportional couplings to all the reservoirs where the linear conductance can be related to the equilibrium spectral density of the dot [20]. To calculate the latter, all reservoirs can be taken together to a single one and only the total tunneling matrix matters. However, when all reservoirs are coupled in a generic way to the dot or when they are characterized by different temperatures or chemical potentials, the analysis of Ref. [16] is no longer valid. This fact was emphasized in Ref. [21], where it was shown that in a generic *nonequilibrium* situation, the proper effective model for $N_{\rm dot} = 1$ and $N = 2$ is a spin-valve model, where the spin polarizations of all reservoirs point in different directions, such that at the low-energy fixed point their sum is equal to zero. This has the consequence that the fixed-point model in nonequilibrium is essentially not SU(2) symmetric and new interesting nonequilibrium fixed-point models emerge with different non-Kondo-type properties in the weak- as well as in the strong-coupling regime. Only in the equilibrium situation when all reservoirs are characterized by the same temperature and chemical potential, all reservoirs can be taken together, resulting in an unpolarized reservoir with SU(2) symmetry at the fixed point. The nonequilibrium properties at and away from the fixed-point model have been studied for large voltages above the Kondo temperature [21], and a smoking gun was identified in the nontrivial magnetic field dependence of the magnetization and the transport current characterizing the fixed-point model.

The proposals of new nonequilibrium fixed-point models are of particular interest for the constant effort to generalize well-established analytical and numerical methods for the study of equilibrium properties of quantum impurity models [3,22] to the nonequilibrium case. Recent developments of perturbative renormalization group methods [23–26] have shown how the voltage dependence and the physics of cutoff scales by decay rates can be implemented [27] and how the time evolution into the stationary state can be calculated [28]. Even in the strong-coupling regime [29,30] results in agreement with experiments [31] were obtained, although the used methods are essentially perturbative and not capable of describing the strong-coupling regime in general. Therefore, numerically exact methods are required for the description of quantum dot systems in nonequilibrium, such as, e.g., the time-dependent numerical renormalization group (TD-NRG) [32], time-dependent density matrix renormalization group (TD-DMRG) [33], iterative stochastic path integrals [34], and quantum Monte Carlo methods [35]. Recently, a promising thermofield approach has been suggested by a combination of TD-NRG and TD-DMRG [36] showing a good agreement with the strong-coupling results for the nonequilibrium Kondo model of Refs. [29–31].

The aim of this paper is to analyze the generic case $N_{\rm dot} = 1$ and arbitrary N to see how the results of Ref. [21] can be generalized to the case $N > 2$. In particular, we will study the case $N = 3$ and, starting from a generic tunneling matrix, will show that an effective tunneling model can be derived where also the reservoirs are characterized by three flavors which we will conveniently label by the up (u), down (d), and strange (s) quark flavors. The effective model in the cotunneling regime of a singly occupied quantum dot can be described by flavor fluctuations, and we will show by a poor man's scaling analysis that the low-energy fixed-point model is indeed the SU(3)-symmetric Kondo model. This result is shown to hold also for arbitrary N within the poor man's scaling analysis and will be explicitly confirmed for $N = 3$ by a numerically exact NRG analysis for the linear response conductance, similiar to Refs. [12,13]. In addition to these references, we will study the dependence of the SU(3) Kondo temperature on the tunneling matrix elements and will show how the SU(3)-symmetric point is obtained by a proper adjustment of the level spacings of the dot. Subsequently, we will analyze the nonequilibrium situation and generalize the spin-valve model of Ref. [21] for $N = 2$ to the case of three levels $N = 3$. In this case, a fixed-point model arises where the reservoirs are characterized by eight-dimensional F spins corresponding to the eight generators of the SU(3) group which cancel when all reservoirs are taken together. For large voltages and two reservoirs we find that the nonequilibrium fixed-point model has a characteristic dependence on the dot parameters for zero F-spin magnetization on the dot providing a *smoking gun* for the detection of the fixed point. Thus, we conclude that the results of Ref. [21] can indeed be generalized to the case of $N > 2$ levels with a great potential for a variety of new interesting nonequilibrium fixed-point models where the low-energy behavior in the strong-coupling regime is still unknown.

The paper is organized as follows. In Sec. II we will derive various effective models. We will set up effective tunneling models in Sec. II A and the effective model in the cotunneling regime in Sec. II B. The fixed-point model is obtained via a poor man's scaling analysis in Sec. II C for arbitrary N. In Sec. II D we consider the particular case $N = 3$ and will set up the relation to the representation of the SU(3) group and the physical picture in terms of F-spin interactions. In Sec. III we will use the NRG method to confirm the SU(3)-symmetric fixed-point model in the linear response regime. Finally, in Sec. IV we analyze the nonequilibrium properties of the fixed-point model in the perturbative regime of large voltage via a Fermi's golden rule approach. The general formulas are derived in Sec. IV A and the magnetization and the current are calculated as function of characteristic dot parameters for the case of two reservoirs in Sec. IV B where the smoking gun for the detection of the fixed-point model is derived. We close with a summary of our results in Sec. V. We use units $e = \hbar = 1$ throughout this paper.

II. DERIVATION OF EFFECTIVE MODELS

In this section we start from a quantum dot with N levels coupled via a generic tunneling matrix to $N_{\rm res}$ multichannel noninteracting reservoirs in grand-canonical equilibrium. We

show in Sec. II A that this model is equivalent to an effective one where the number of channels in each reservoir is the same as the number N of the quantum dot levels. For the special case of $N = 3$ this sets the basis to use a notation in terms of three flavor states for the three channels and to characterize the reservoirs by rotated F spins with a certain isospin and hypercharge polarization. In addition, we will set up various effective tunneling models and characterize the properties of the central fixed-point model derived in Secs. II B–II D for the cotunneling regime, where the number $N_{\rm dot}$ of particles on the dot is fixed to $N_{\rm dot} = 1$, such that only flavor fluctuations via virtual intermediate states can occur. In this regime, we will derive an effective model describing flavor fluctuations and propose the fixed-point model from a poor man's scaling analysis.

A. Effective tunneling models

The starting point is a quantum dot consisting of N levels characterized by some quantum number $l = 1,2,\ldots,N$, together with a Coulomb energy $E_{N_{\rm dot}}$ depending only on the total particle number operator $N_{\rm dot} = \sum_l c_l^\dagger c_l$ of the dot

$$H_{\rm dot} = \sum_{ll'} h_{ll'} c_l^\dagger c_{l'} + E_{N_{\rm dot}}, \tag{1}$$

$$E_{N_{\rm dot}} = E_C (N_{\rm dot} - n_x)^2, \tag{2}$$

where $c_l^\dagger / c_l$ are the creation/annihilation operators of the single-particle states of the dot. The charging energy E_c is assumed to be the largest energy scale in the problem such that, for small $h_{ll'}$, the parameter n_x determines the occupation of the dot. If $n_x = n$ is integer, the ground state will be dominated by $N_{\rm dot} = n$, whereas for half-integer $n_x = n + \frac{1}{2}$, states with $N_{\rm dot} = n, n+1$ are degenerate with respect to the Coulomb interaction. For convenience, we define the gate voltage by

$$V_g = E_c (2n_x - N), \tag{3}$$

such that $V_g = 0$ (or $n_x = N/2$) defines the particle-hole-symmetric point for $h_{ll'} = 0$. With this definition we can also write the dot Hamiltonian in second quantized form as

$$H_{\rm dot} = \sum_{ll'} \tilde{h}_{ll'} c_l^\dagger c_{l'} + \frac{U}{2} \sum_{ll'} c_l^\dagger c_{l'}^\dagger c_{l'} c_l, \tag{4}$$

with $U = 2E_c$ and $\tilde{h}_{ll'} = h_{ll'} - [V_g + (U/2)(N-1)]\delta_{ll'}$.

The quantum dot is coupled via a generic tunneling matrix to several infinitely large reservoirs $\alpha = 1,2,\ldots,N_{\rm res}$ kept at grand-canonical equilibrium with temperature T and chemical potential μ_α, such that the total Hamiltonian reads as

$$H_{\rm tot} = H_{\rm dot} + H_{\rm res} + H_T, \tag{5}$$

with the reservoir Hamiltonian

$$H_{\rm res} = \sum_{\alpha \nu_\alpha k} \epsilon_{\alpha\nu_\alpha k}\, a_{\alpha\nu_\alpha k}^\dagger a_{\alpha\nu_\alpha k}, \tag{6}$$

and the tunneling Hamiltonian

$$H_T = \frac{1}{\sqrt{\rho^{(0)}}} \sum_{\alpha\nu_\alpha lk} \left\{ t_{\nu_\alpha l}^\alpha a_{\alpha\nu_\alpha k}^\dagger c_l + \left(t_{\nu_\alpha l}^\alpha\right)^* c_l^\dagger a_{\alpha\nu_\alpha k} \right\}. \tag{7}$$

Here, $\nu_\alpha = 1,2,\ldots,N_\alpha$ is the channel index for reservoir α (with N_α channels in total), $\epsilon_{\alpha\nu_\alpha k}$ is the band dispersion of reservoir α for channel ν_α relative to the chemical potential μ_α and labeled by k (which becomes continuous in the thermodynamic limit), and $t_{\nu_\alpha l}^\alpha$ is the tunneling matrix between the dot and reservoir α. $\rho^{(0)}$ is some average density of states (DOS) in the reservoirs, which is set to $\rho^{(0)} = 1$ in the following defining the energy units. In vector-matrix notation, the tunneling Hamiltonian can be written in a more compact form as

$$H_T = \sum_{\alpha k} \{ \underline{a}_{\alpha k}^\dagger \underline{\underline{t}}_\alpha \underline{c} + \underline{c}^\dagger \underline{\underline{t}}_\alpha^\dagger \underline{a}_{\alpha k} \}, \tag{8}$$

where $\underline{c}^\dagger = (c_1^\dagger, \ldots, c_N^\dagger)$, $\underline{a}_{\alpha k}^\dagger = (a_{\alpha 1 k}^\dagger, \ldots, a_{\alpha N_\alpha k}^\dagger)$, and $\underline{\underline{t}}_\alpha$ is a $N_\alpha \times N$ matrix with matrix elements $t_{\nu_\alpha l}^\alpha$. For convenience, we have taken here a tunneling matrix independent of k which is usually a very good approximation for rather flat reservoir bands on the scale of the low-energy scales of interest.

Using Keldysh formalism. it is straightforward [20,37] to relate the stationary current $I_{\alpha\nu_\alpha}$ in reservoir α and channel ν_α to the stationary nonequilibrium greater/lesser Green's functions $G_{ll'}^{\gtrless}(\omega)$ of the dot via

$$I_{\alpha\nu_\alpha} = \frac{e}{h} \int d\omega\, {\rm Tr}\, \underline{\underline{\Gamma}}_{\alpha\nu_\alpha} \{ [1 - f_\alpha(\omega)]\, i\underline{\underline{G}}^<(\omega) + f_\alpha(\omega)\, i\underline{\underline{G}}^>(\omega) \}, \tag{9}$$

where Tr denotes the trace over the single-particle states of the dot, $f_\alpha(\omega) = (e^{\beta(\omega-\mu_\alpha)} + 1)^{-1}$ is the Fermi function of reservoir α, and the $(N \times N)$-hybridization matrix $\underline{\underline{\Gamma}}_{\alpha\nu_\alpha}$ is defined by

$$\left(\underline{\underline{\Gamma}}_{\alpha\nu_\alpha}\right)_{ll'} = 2\pi \rho_{\alpha\nu_\alpha} \left(t_{\nu_\alpha l}^\alpha\right)^* t_{\nu_\alpha l'}^\alpha. \tag{10}$$

Here, $\rho_{\alpha\nu_\alpha} = \sum_k \delta(\omega - \epsilon_{\alpha\nu_\alpha k})$ denotes the DOS in reservoir α for channel ν_α, which is assumed to be rather flat so that the energy dependence can be neglected. The influence of the reservoirs and the tunneling on the Green's functions is determined by the reservoir part of the lesser/greater self-energy given by

$$\underline{\underline{\Sigma}}_{\rm res}^<(\omega) = i \sum_\alpha f_\alpha(\omega) \underline{\underline{\Gamma}}_\alpha, \tag{11}$$

$$\underline{\underline{\Sigma}}_{\rm res}^>(\omega) = -i \sum_\alpha (1 - f_\alpha(\omega)) \underline{\underline{\Gamma}}_\alpha, \tag{12}$$

where

$$\underline{\underline{\Gamma}}_\alpha = \sum_{\nu_\alpha} \underline{\underline{\Gamma}}_{\alpha\nu_\alpha} = 2\pi\, \underline{\underline{t}}_\alpha^\dagger\, \underline{\underline{\rho}}_\alpha\, \underline{\underline{t}}_\alpha \tag{13}$$

is the hybridization matrix for reservoir α including all channels and $(\underline{\underline{\rho}}_\alpha)_{\nu_\alpha\nu_\alpha'} = \delta_{\nu_\alpha\nu_\alpha'}\rho_{\alpha\nu_\alpha}$ is the diagonal matrix for the DOS of reservoir α. As a consequence, we see that the Green's functions depend on the reservoirs and the tunneling matrix only via the hybridization matrices $\underline{\underline{\Gamma}}_\alpha$ of all the reservoirs. Thus, two models with the same hybridization matrices give exactly the same Green's functions. Once the Green's functions are known, the channel-resolved currents $I_{\alpha\nu_\alpha}$ can be calculated from (9), where the channel-resolved hybridization matrix $\underline{\underline{\Gamma}}_{\alpha\nu_\alpha}$ of the concrete model under consideration has to be

inserted. The stationary expectation values of single-particle operators of the dot can be directly calculated from the lesser Green's functions via $\langle c_{l'}^\dagger c_l\rangle = \frac{1}{2\pi i}\int d\omega\, G^<_{ll'}(\omega)$ and thus are exactly the same for two models with the same hybridization matrices $\underline{\underline{\Gamma}}_\alpha$.

We note that for the equilibrium case, where all Fermi functions of the reservoirs are the same, the reservoir self-energies involve only the total hybridization matrix

$$\underline{\underline{\Gamma}} = \sum_\alpha \underline{\underline{\Gamma}}_\alpha, \tag{14}$$

with the result that the equilibrium Green's functions are the same for two models with the same $\underline{\underline{\Gamma}}$. However, the current in linear response can not be related to the single-particle Green's functions in equilibrium via (9) since also the Green's functions have to be expanded in the voltages. A special case is the one of proportional couplings where it is assumed that $\underline{\underline{\Gamma}}_\alpha = x_\alpha \underline{\underline{\Gamma}}$ with $\sum_\alpha x_\alpha = 1$. Using current conservation $\sum_\alpha I_\alpha = 0$, with $I_\alpha = \sum_{\nu_\alpha} I_{\alpha\nu_\alpha}$ denoting the total current in reservoir α, we get in this case from (9) the Landauer-Büttiker–type formula [20]

$$I_\alpha = \frac{e}{h}\sum_{\beta\neq\alpha}\int d\omega\, T_{\alpha\beta}(\omega)(f_\alpha - f_\beta)(\omega), \tag{15}$$

with the transmission probability

$$T_{\alpha\beta}(\omega) = 2\pi\, x_\alpha x_\beta \mathrm{Tr}\, \underline{\underline{\Gamma}}\, \underline{\underline{\rho}}(\omega), \tag{16}$$

where $\underline{\underline{\rho}}(\omega) = \frac{i}{2\pi}(\underline{\underline{G}}^R - \underline{\underline{G}}^A)(\omega)$ is the spectral density on the dot. From this formula one can see that in linear response, where $(f_\alpha - f_\beta)(\omega) \approx -f'(\omega)(\mu_\alpha - \mu_\beta)$, one needs only the spectral density in equilibrium and, with $\mu_\alpha = -eV_\alpha$, the current can be written as

$$I_\alpha = \sum_\beta G_{\alpha\beta}(V_\beta - V_\alpha), \tag{17}$$

with the conductance tensor

$$G_{\alpha\beta} = -\frac{e^2}{h}\int d\omega\, T_{\alpha\beta}(\omega)\, f'(\omega). \tag{18}$$

With the knowledge that the hybridization matrices $\underline{\underline{\Gamma}}_\alpha$ are the only input we need to characterize the reservoirs and the tunneling matrix, we can now proceed to define effective models with the same hybridization matrices. Since $\underline{\underline{\Gamma}}_\alpha$ is a positive-definite Hermitian matrix, we can diagonalize it with a unitary matrix $\underline{\underline{U}}_\alpha$,

$$\underline{\underline{\Gamma}}_\alpha = \underline{\underline{U}}_\alpha\, \underline{\underline{\Gamma}}^{\mathrm{d}}_\alpha\, \underline{\underline{U}}^\dagger_\alpha, \tag{19}$$

where $(\underline{\underline{\Gamma}}^{\mathrm{d}}_\alpha)_{ll'} = \delta_{ll'}\Gamma_{\alpha l}$ is a diagonal matrix with positive eigenvalues $\Gamma_{\alpha l} = 2\pi t_{\alpha l}^2 > 0$. We exclude here the exotic case that one of the eigenvalues $\Gamma_{\alpha l}$ is zero since this would mean that one of the reservoir channels effectively decouples from the system. Following Ref. [21], we can write the hybridization matrix in two equivalent forms by shifting the whole information either to an effective tunneling matrix or to an effective DOS of the reservoirs. In the first case, we introduce an effective tunneling matrix $\underline{\underline{t}}^{\mathrm{eff}}_\alpha$ by

$$\left(\underline{\underline{t}}^{\mathrm{eff}}_\alpha\right)_{ll'} = t_{\alpha l}(\underline{\underline{U}}^\dagger_\alpha)_{ll'} \tag{20}$$

and get

$$\underline{\underline{\Gamma}}_\alpha = 2\pi\left(\underline{\underline{t}}^{\mathrm{eff}}_\alpha\right)^\dagger \underline{\underline{t}}^{\mathrm{eff}}_\alpha. \tag{21}$$

Since $\underline{\underline{t}}^{\mathrm{eff}}_\alpha$ is an $N\times N$ matrix, this effective model consists of reservoirs which have exactly the same number N of channels as we have levels on the dot, i.e., the quantum number on the dot is also the quantum number labeling the channels in the effective reservoirs but this quantum number is in general not conserved by tunneling. Comparing (21) to (13), we see that the effective DOS in the reservoirs is unity, i.e., we consider unpolarized reservoirs.

In the second case, we define an effective DOS $\underline{\underline{\rho}}^{\mathrm{eff}}_\alpha$ in reservoir α by

$$\underline{\underline{\rho}}^{\mathrm{eff}}_\alpha = N\,\underline{\underline{U}}_\alpha\left(\underline{\underline{\Gamma}}^d_\alpha/\Gamma_\alpha\right)\underline{\underline{U}}^\dagger_\alpha, \tag{22}$$

with $\Gamma_\alpha = \sum_l \Gamma_{\alpha l}$. Defining an average tunneling matrix element $t_\alpha > 0$ by $t_\alpha^2 = \frac{1}{N}\sum_l t_{\alpha l}^2$, we can then write the hybridization matrix as

$$\underline{\underline{\Gamma}}_\alpha = 2\pi t_\alpha^2\, \underline{\underline{\rho}}^{\mathrm{eff}}_\alpha. \tag{23}$$

In this case, the effective tunneling matrix is proportional to unity, the tunneling conserves the flavor and is flavor independent. In contrast, the effective DOS contains the whole nontrivial information of the hybridization matrix and describes a unitary transformation of the diagonal matrix $N\,\underline{\underline{\Gamma}}^{\mathrm{d}}_\alpha/\Gamma_\alpha$. The latter matrix can be decomposed in a basis of all diagonal matrices and the coefficients can be interpreted as physical parameters characterizing the effective reservoirs. Using $\mathrm{Tr}\,\underline{\underline{\Gamma}}^{\mathrm{d}}_\alpha = \Gamma_\alpha$, we get for $N = 2$

$$2\,\underline{\underline{\Gamma}}^d_\alpha/\Gamma_\alpha = \underline{\underline{\mathbb{1}}}_2 + p_\alpha \underline{\underline{\sigma}}_z, \tag{24}$$

where σ_z is the Pauli matrix in the z direction and p_α describes the spin polarization in reservoir α. Since the matrix has only positive diagonal elements we get the condition $-1 < p_\alpha < 1$. If one orders the eigenvalues according to $\Gamma_{\alpha 1} \geqslant \Gamma_{\alpha 2}$, one gets $0 < p_\alpha < 1$.

For $N = 3$ we obtain

$$3\,\underline{\underline{\Gamma}}^{\mathrm{d}}_\alpha/\Gamma_\alpha = \underline{\underline{\mathbb{1}}}_3 + p_\alpha \underline{\underline{\lambda}}_3 + \frac{q_\alpha}{\sqrt{3}}\underline{\underline{\lambda}}_8, \tag{25}$$

where

$$\underline{\underline{\lambda}}_3 = \begin{pmatrix} 1 & 0 & 0\\ 0 & -1 & 0\\ 0 & 0 & 0\end{pmatrix}, \tag{26}$$

$$\underline{\underline{\lambda}}_8 = \frac{1}{\sqrt{3}}\begin{pmatrix} 1 & 0 & 0\\ 0 & 1 & 0\\ 0 & 0 & -2\end{pmatrix} \tag{27}$$

are the two diagonal generators of the SU(3) group, describing the isospin in z direction of the up/down quark and the hypercharge operator $\underline{\underline{Y}} = \frac{1}{\sqrt{3}}\underline{\underline{\lambda}}_8$, respectively. Therefore, we interpret p_α as the isospin polarization and q_α as the hypercharge polarization characterizing the reservoirs in the three-channel case. The fact that all matrix elements of (25) are positive leads to the two conditions

$$|p_\alpha| < 1 + \frac{q_\alpha}{3}, \quad 0 < 1 + \frac{q_\alpha}{3} < \frac{3}{2}. \tag{28}$$

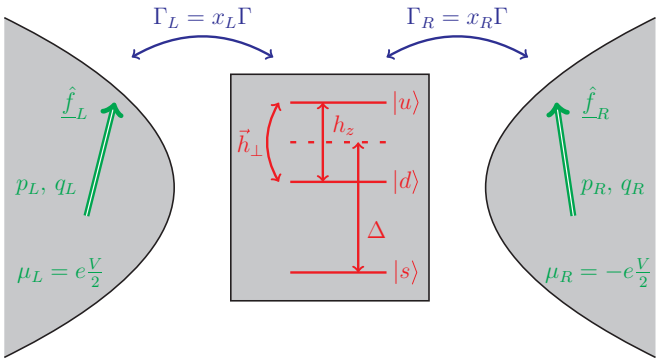

FIG. 1. Sketch of the effective model of two F-spin polarized leads $\alpha = L,R$ coupled to a three-level quantum dot via flavor-conserving tunneling rates $\Gamma_{L,R} = x_{L,R}\Gamma$. $\mu_{L,R} = \pm eV/2$ denote the chemical potentials of the leads with eight-dimensional F spins $\underline{f}_{L,R}$ characterized by an isospin polarization $p_{L,R}$ and hypercharge polarization $q_{L,R}$. $\vec{h} = (\vec{h}_\perp, h_z)$ with $\vec{h}_\perp = (h_x, h_y)$ denotes the magnetic field acting on the two isospin dot levels (up and down quarks), and Δ is the level spacing between the strange quark and the average of the two isospin levels.

If one orders the eigenvalues according to $\Gamma_{\alpha 1} \geqslant \Gamma_{\alpha 2} \geqslant \Gamma_{\alpha 3}$, one gets $0 < p_\alpha < q_\alpha < \frac{3}{2}$.

The unitary transformation $\underline{\underline{U}}_\alpha$ describes a rotation of the direction of the spin-$\frac{1}{2}$ in the $N = 2$ case, and a rotation of the eight-dimensional F spin with $\underline{\underline{F}}_i = \frac{1}{2}\underline{\underline{\lambda}}_i$ for $N = 3$ (see Fig. 1 for an illustration). Thus, the form (23) allows for a nice physical interpretation in terms of physical parameters characterizing the reservoirs. For $N = 3$, we can label the three flavors of the reservoirs and the dot by $l = u,d,s$ for the up, down, and strange quark and describe with the form (23) a system where the flavor is conserved in tunneling with equal tunneling amplitudes for all flavors. However, the polarization p_α of the isospin described by the up and down quarks and the hypercharge polarization q_α can be different for each reservoir, and the F spins in the reservoirs can all be rotated relative to the F spin of the dot. This naturally generalizes the effective spin-valve model set up in Ref. [21] for $N = 2$ to the $N = 3$ case, which is the main subject of this paper.

The form (21) in terms of an effective tunneling matrix allows for another representation of the hybridization matrix which will turn out to be crucial to interpret the fixed-point model derived in Sec. II C for the cotunneling regime. Taking all effective tunneling matrices together in a $N \cdot N_{\rm res} \times N$ matrix

$$\underline{t}^{\rm eff} = \begin{pmatrix} \underline{\underline{t}}^{\rm eff}_1 \\ \cdot \\ \cdot \\ \cdot \\ \underline{\underline{t}}^{\rm eff}_{N_{\rm res}} \end{pmatrix}, \tag{29}$$

we can write this matrix via a singular value decomposition as

$$\underline{t}^{\rm eff} = \underline{\underline{V}} \begin{pmatrix} \underline{\underline{\gamma}} \\ 0 \end{pmatrix} \underline{\underline{W}}^\dagger, \tag{30}$$

where $\underline{\underline{V}}$ is a unitary $N \cdot N_{\rm res} \times N \cdot N_{\rm res}$ matrix, $\underline{\underline{\gamma}}$ is an $N \times N$ diagonal matrix containing the positive singular values $\gamma_1 \geqslant \gamma_2 \geqslant \cdots \geqslant \gamma_N > 0$, and $\underline{\underline{W}}$ is a unitary $N \times N$ matrix. We assume here that N singular values exist, excluding exotic cases where some channels decouple effectively from the system. As a consequence, we can express all effective tunneling matrices in terms of the singular value matrix $\underline{\underline{\gamma}}$ as follows:

$$\underline{\underline{t}}^{\rm eff}_\alpha = \underline{\underline{V}}_\alpha \, \underline{\underline{\gamma}} \, \underline{\underline{W}}^\dagger, \tag{31}$$

where $\underline{\underline{V}}_\alpha$ are the $N \times N$ matrices occurring in the first N columns of $\underline{\underline{V}}$, which are in general *not* unitary. However, since $\underline{\underline{V}}$ is unitary, we note the important property

$$\sum_\alpha \underline{\underline{V}}^\dagger_\alpha \, \underline{\underline{V}}_\alpha = \underline{\underline{\mathbb{1}}}. \tag{32}$$

The unitary matrix $\underline{\underline{W}}$ can be eliminated by transforming the basis of the single-particle states of the dot using new field operators $\underline{c}' = \underline{\underline{W}}^\dagger \underline{c}$, such that the dot Hamiltonian (1) and the tunneling Hamiltonian (8) obtain the form

$$H_{\rm dot} = (\underline{c}')^\dagger \underline{\underline{h}}' \underline{c}' + E_{N_{\rm dot}}, \tag{33}$$

$$H_T = \sum_{\alpha k} \left\{ \underline{a}^\dagger_{\alpha k} \left(\underline{\underline{t}}^{\rm eff}_\alpha\right)' \underline{c}' + (\underline{c}')^\dagger \left(\left(\underline{\underline{t}}^{\rm eff}_\alpha\right)'\right)^\dagger \underline{a}_{\alpha k} \right\}, \tag{34}$$

with $\underline{\underline{h}}' = \underline{\underline{W}}^\dagger \, \underline{\underline{h}} \, \underline{\underline{W}}$ and

$$\left(\underline{\underline{t}}^{\rm eff}_\alpha\right)' = \underline{\underline{V}}_\alpha \, \underline{\underline{\gamma}}. \tag{35}$$

For simplicity, we will drop the prime in the following and replace $\underline{\underline{h}}' \to \underline{\underline{h}}$ and $(\underline{\underline{t}}^{\rm eff}_\alpha)' \to \underline{\underline{t}}^{\rm eff}_\alpha$ keeping in mind that these matrices result from the matrices of the original model by transforming the dot channels with the unitary matrix $\underline{\underline{W}}$.

In terms of the effective tunneling matrices (35), the hybridization matrices (21) obtain the form

$$\underline{\underline{\Gamma}}_\alpha = 2\pi \, \underline{\underline{\gamma}} \, \underline{\underline{V}}^\dagger_\alpha \, \underline{\underline{V}}_\alpha \, \underline{\underline{\gamma}}. \tag{36}$$

This form is of particular interest since it separates the hybridization matrix in a part $\underline{\underline{\gamma}}$ which is independent of the reservoirs and a reservoir-dependent part $\underline{\underline{V}}^\dagger_\alpha \, \underline{\underline{V}}_\alpha$. Comparing (36) with (13), we can interpret $\underline{\underline{\gamma}}$ as an effective tunneling matrix which conserves the flavor index and is the same for all reservoirs. This effective tunneling matrix contains the information of the eigenvalues $\Gamma_l = 2\pi\gamma_l^2$ of the total hybridization matrix since we get from (32)

$$\underline{\underline{\Gamma}} = \sum_\alpha \underline{\underline{\Gamma}}_\alpha = 2\pi \, \underline{\underline{\gamma}}^2. \tag{37}$$

The reservoir-dependent part $\underline{\underline{V}}^\dagger_\alpha \, \underline{\underline{V}}_\alpha$ can be interpreted as an effective DOS of the reservoirs. Taking $N = 3$ and decomposing this Hermitian matrix in the basis of the F-spin generators $\underline{\underline{F}}_i = \frac{1}{2}\underline{\underline{\lambda}}_i$ of SU(3) we get

$$\underline{\underline{V}}^\dagger_\alpha \, \underline{\underline{V}}_\alpha = x_\alpha \left(\underline{\underline{\mathbb{1}}} + \sum_{i=1}^{8} d^i_\alpha \, \underline{\underline{F}}_i \right), \tag{38}$$

with real coefficients x_α and d^i_α which, due to (32), fulfill the property

$$\sum_\alpha x_\alpha = 1, \quad \sum_\alpha x_\alpha d^i_\alpha = 0. \tag{39}$$

This means that the sum of the F spins of all reservoirs is zero. A similiar property holds for arbitrary N. In equilibrium, where all chemical potentials $\mu_\alpha = \mu$ are the same and all reservoirs can be taken together to one big reservoir, this means that an unpolarized reservoir with SU(3) symmetry couples to the dot. However, since the effective tunneling matrix elements γ_l still depend on the flavor index, SU(3) symmetry does not hold for the total system even in equilibrium.

Most importantly, we will see in Sec. II C by a poor man's scaling analysis in the cotunneling regime of a singly occupied dot $N_{\rm dot} = 1$ that a generic fixed-point model with an isotropic matrix $\underline{\underline{\gamma}} = \gamma \underline{\underline{\mathbb{1}}}$ emerges, such that the effective tunneling matrix (35) reads as

$$\underline{\underline{t}}^{\rm eff}_\alpha = \gamma \underline{\underline{V}}_\alpha. \tag{40}$$

$\gamma > 0$ can be related to an isotropic Kondo coupling J via

$$\gamma^2 = \frac{1}{4} J D, \quad \frac{1}{D} = \frac{1}{2}\left(\frac{1}{E_0} + \frac{1}{E_2}\right), \tag{41}$$

where $E_{N_{\rm dot}}$ is given by (2) and J fulfils the poor man's scaling equation

$$\frac{dJ}{d\Lambda} = -\frac{N}{2}\frac{J^2}{\Lambda}, \tag{42}$$

with Λ denoting the effective bandwidth. In addition, a special potential scattering term emerges in the original tunneling model at the fixed point which is given by

$$V_{\rm sc} = v_{\rm sc} \sum_{kk'} \sum_{\alpha\alpha'} : \underline{a}^\dagger_{\alpha k} \underline{\underline{V}}_\alpha \underline{\underline{V}}^\dagger_{\alpha'} \underline{a}_{\alpha' k'} : , \tag{43}$$

where

$$v_{\rm sc} = \frac{\gamma^2}{D}\left(\frac{N-2}{N} + \delta\right), \quad \delta = \frac{E_0 - E_2}{E_2 + E_0}, \tag{44}$$

with E_0 and E_2 from (2), and $: \cdots :$ denotes normal ordering. This potential scattering term vanishes for $N = 2$ and $\delta = 0$ (i.e., $n_x = 1$ where $E_0 = E_2$) and is such that it cancels the potential scattering term emerging in an effective model for the cotunneling regime (see Sec. II B). Due to $V_{\rm sc}$, the reservoir part of the self-energy of the dot is more complicated than (11) and (12) and does not only depend on the hybridization matrix. However, as is shown in Appendix A, the effect of $V_{\rm sc}$ is just that γ is changed to an effective $\tilde{\gamma}$ given by

$$\tilde{\gamma} = \frac{\gamma}{\sqrt{1 + \pi^2 v_{\rm sc}^2}}, \tag{45}$$

such that the self-energies (11) and (12) from the reservoirs can be written at the fixed point with effective hybridization matrices which can be either expressed via an effective tunneling matrix analog to (21):

$$\underline{\underline{\Gamma}}_\alpha = 2\pi \left(\underline{\underline{t}}^{\rm eff}_\alpha\right)^\dagger \underline{\underline{t}}^{\rm eff}_\alpha, \quad \underline{\underline{t}}^{\rm eff}_\alpha = \tilde{\gamma} \underline{\underline{V}}_\alpha, \tag{46}$$

such that the DOS of the reservoirs is unity, or via an effective DOS analog to (23),

$$\underline{\underline{\Gamma}}_\alpha = 2\pi \tilde{\gamma}^2 \underline{\underline{\rho}}^{\rm eff}_\alpha, \quad \underline{\underline{\rho}}^{\rm eff}_\alpha = \underline{\underline{V}}^\dagger_\alpha \underline{\underline{V}}_\alpha, \tag{47}$$

with a trivial tunneling matrix given by $\tilde{\gamma}\underline{\underline{\mathbb{1}}}$ which is the same for all reservoirs and proportional to unity with respect to the flavor indices. The particular property of the effective DOS at the fixed point is the condition

$$\sum_\alpha \underline{\underline{\rho}}^{\rm eff}_\alpha = \underline{\underline{\mathbb{1}}}, \tag{48}$$

following from (32). This means that in contrast to the general case depicted in Fig. 1 for $N = 3$, the particular property of the fixed-point model is that the sum over all reservoir F spins is equal to zero *and* the tunneling matrix $\underline{\underline{\gamma}} = \gamma\underline{\underline{\mathbb{1}}}$ is isotropic. As a consequence, we get overall SU(3) symmetry in equilibrium, whereas in nonequilibrium the fixed-point model is essentially *not* SU(3) symmetric since the F spins of the reservoirs are nonzero. A similar statement holds for any number N of dot levels, generalizing the picture found in Ref. [21] for $N = 2$ to a generic multilevel quantum dot.

We note that for the particular case of two reservoirs $N_{\rm res} = 2$ with $\alpha = L, R$, we get from (32) that $\underline{\underline{V}}^\dagger_L \underline{\underline{V}}_L = \underline{\underline{\mathbb{1}}} - \underline{\underline{V}}^\dagger_R \underline{\underline{V}}_R$, such that we can find a common unitary matrix $\underline{\underline{U}}_V$ which diagonalizes both $\underline{\underline{V}}^\dagger_\alpha \underline{\underline{V}}_\alpha$ for $\alpha = L, R$

$$\underline{\underline{V}}^\dagger_\alpha \underline{\underline{V}}_\alpha = \underline{\underline{U}}_V \underline{\underline{A}}^{\rm d}_\alpha \underline{\underline{U}}^\dagger_V, \tag{49}$$

where $\underline{\underline{A}}^{\rm d}_\alpha$ are diagonal matrices with the property

$$\sum_{\alpha = L,R} \underline{\underline{A}}^{\rm d}_\alpha = \underline{\underline{\mathbb{1}}}. \tag{50}$$

For $N = 3$, the matrix $\underline{\underline{A}}^{\rm d}_\alpha$ can be decomposed analog to (25) as

$$\underline{\underline{A}}^{\rm d}_\alpha = x_\alpha \left(\underline{\underline{\mathbb{1}}}_3 + p_\alpha \underline{\underline{\lambda}}_3 + \frac{q_\alpha}{\sqrt{3}} \underline{\underline{\lambda}}_8\right), \tag{51}$$

where, due to the property (50), we get

$$1 = x_L + x_R, \tag{52}$$

$$0 = x_L p_L + x_R p_R, \tag{53}$$

$$0 = x_L q_L + x_R q_R, \tag{54}$$

together with $0 < x_\alpha < 1$ and (28). Thus, the hybridization matrices at the fixed point obtain the following form for two reservoirs:

$$\underline{\underline{\Gamma}}_\alpha = 2\pi \tilde{\gamma}^2 \underline{\underline{U}}_V \underline{\underline{A}}^{\rm d}_\alpha \underline{\underline{U}}^\dagger_V. \tag{55}$$

Omitting the unitary matrix $\underline{\underline{U}}_V$ by choosing a different single-particle basis for the dot states and redefining the parameters $h_{ll'}$ [analog to the transformation by the unitary matrix $\underline{\underline{W}}$, see (33) and (34)], we get finally the diagonal form

$$\underline{\underline{\Gamma}}_\alpha = 2\pi \tilde{\gamma}^2 \underline{\underline{A}}^{\rm d}_\alpha, \tag{56}$$

which, for $N = 3$, by inserting the decomposition (51), can be written as

$$\underline{\underline{\Gamma}}_{\alpha} = \frac{1}{3}\Gamma_{\alpha}\left(\underline{\underline{\mathbb{1}}}_3 + p_{\alpha}\underline{\underline{\lambda}}_3 + \frac{q_{\alpha}}{\sqrt{3}}\underline{\underline{\lambda}}_8\right), \tag{57}$$

with $\Gamma_{\alpha} = 2\pi\tilde{\gamma}^2 x_{\alpha}$. This form for the hybridization matrices constitutes the central generic fixed-point model for $N = 3$ and two reservoirs in the cotunneling regime of a singly occupied dot. This will be confirmed in Sec. III by NRG in equilibrium and analyzed in Sec. IV by a golden rule approach in nonequilibrium. It generalizes the spin-valve model for a two-level quantum dot with opposite spin polarizations in the two reservoirs analyzed in Ref. [21] to the case of a three-level quantum dot, where the isospin and hypercharge polarizations have to be opposite in the two reservoirs. An analog fixed-point model arises for an arbitrary number of dot levels, in this case one obtains in the two reservoirs opposite parameters corresponding to the $N-1$ diagonal generators of SU(N). Whereas in equilibrium the fixed-point model is SU(N) symmetric (at least if the dot parmeters $h_{ll'}$ are adjusted properly, see Sec. III) and leads generically to the SU(N) Kondo effect, the nonequilibrium fixed-point model is *not* SU(N) symmetric and generically non-Kondo physics has to be expected. This will be analyzed in Sec. IV in the perturbative golden rule regime of large voltage, where we will see that zero F-spin magnetization on the dot occurs only for particular values of the dot parameters $h_{ll'}$ providing a *smoking gun* for the detection of the fixed-point model.

B. Effective model in the cotunneling regime

The effective model in the cotunneling regime where the particle number on the dot is fixed to $N_{\rm dot} = 1$ can easily be obtained by projecting the Hamiltonian matrix on this subspace analog to Brillouin-Wigner perturbation theory. Taking only one virtual process into the particle number sectors $N_{\rm dot} = 0,2$ into account we get

$$H^{\rm eff}_{\rm tot} = H_{\rm res} + P_1 H_{\rm dot} P_1 - :P_1 H_T Q_1 \frac{1}{H_{\rm dot}} Q_1 H_T P_1:, \tag{58}$$

where P_1 projects onto the one-particle subspace of the dot and $Q_1 = 1 - P_1$. We have introduced the normal-ordering $:\cdots:$ with respect to the reservoir field operators since we are not interested in terms renormalizing the dot Hamiltonian leading to effective parameters $h_{ll'}$. For $H_{\rm res}$ and H_T, we take a model with the effective tunneling matrix (35) and the unity matrix for the effective DOS in the reservoirs, as has been discussed in Sec. II. Inserting $H_{\rm dot}$ and H_T from (1) and (8) and using $E_{N_{\rm dot}}$ from (2) we get with $P_1 c_l^{\dagger} c_{l'} P_1 = |l\rangle\langle l'|$:

$$H^{\rm eff}_{\rm tot} = H_{\rm res} + \sum_{ll'} h_{ll'}|l\rangle\langle l'| + E_1$$
$$- \frac{1}{E_2}\sum_{\alpha\alpha'}\sum_{kk'} :P_1 \underline{a}^{\dagger}_{\alpha k}\underline{\underline{t}}^{\rm eff}_{\alpha}\underline{c}\,\underline{c}^{\dagger}\left(\underline{\underline{t}}^{\rm eff}_{\alpha'}\right)^{\dagger}\underline{a}_{\alpha' k'}P_1: \tag{59}$$
$$- \frac{1}{E_0}\sum_{\alpha\alpha'}\sum_{kk'} :P_1\underline{c}^{\dagger}\left(\underline{\underline{t}}^{\rm eff}_{\alpha'}\right)^{\dagger}\underline{a}_{\alpha' k'}\underline{a}^{\dagger}_{\alpha k}\underline{\underline{t}}^{\rm eff}_{\alpha}\underline{c}P_1:. \tag{60}$$

Using

$$P_1(\underline{c}\,\underline{c}^{\dagger})_{ll'}P_1 = -|l'\rangle\langle l| + \delta_{ll'}P_1,$$
$$:(\underline{a}_{\alpha' k'}\,\underline{a}^{\dagger}_{\alpha k})_{l'l}: = -:a^{\dagger}_{\alpha l k}a_{\alpha' l' k'}:, \tag{61}$$

we get after inserting (35) for the tunneling matrix and leaving out the unimportant constant E_1

$$H^{\rm eff}_{\rm tot} = H_{\rm res} + \sum_{ll'} h_{ll'}|l\rangle\langle l'| + V_{\rm eff}, \tag{62}$$

with the effective interaction

$$V_{\rm eff} = \sum_{\alpha\alpha'}\sum_{kk'} :\underline{a}^{\dagger}_{\alpha k}\underline{\underline{V}}_{\alpha}\underline{\underline{\hat{J}}}\,\underline{\underline{V}}^{\dagger}_{\alpha'}\underline{a}_{\alpha' k'}: \tag{63}$$

and

$$\hat{J}_{ll'} = \gamma_l\gamma_{l'}\left(\frac{2}{D}|l'\rangle\langle l| - \frac{1}{E_2}\delta_{ll'}\hat{\mathbb{1}}\right), \tag{64}$$

with $2/D = 1/E_0 + 1/E_2$ [see (41)]. We note that the hat on $\hat{J}_{ll'}$ indicates that this object is a dot operator in the one-particle subspace for *each* fixed value of l and l', i.e., $\underline{\underline{\hat{J}}}$ represents a $N \times N$ matrix with dot operators in each matrix element. By using $\hat{\mathbb{1}} = \sum_l |l\rangle\langle l|$, a straightforward calculation leads to the decomposition

$$\hat{J}_{ll'} = \xi_{ll'}|l'\rangle\langle l|(1-\delta_{ll'})$$
$$+ \sum_{l_1\neq l}\eta_{ll_1}\left(\frac{1}{N}\hat{\mathbb{1}} - |l_1\rangle\langle l_1|\right)\delta_{ll'} + v_l\delta_{ll'}\hat{\mathbb{1}}, \tag{65}$$

with

$$\xi_{ll'} = \frac{2}{D}\gamma_l\gamma_{l'}, \quad \eta_{ll'} = \frac{2}{D}\gamma_l^2, \tag{66}$$
$$v_l = -\frac{1}{D}\gamma_l^2\left(\frac{N-2}{N} + \delta\right), \tag{67}$$

and $2\delta = D/E_2 - D/E_0$ [see (44)]. We note that the bare parameters $\eta_{ll'}$ are independent of l' but obtain a strong dependence on l' under the renormalization group flow described below. The decomposition (65) exhibits the nondiagonal matrix $|l'\rangle\langle l|$ for $l \neq l'$, all traceless diagonal matrices $\frac{1}{N}\hat{\mathbb{1}} - |l_1\rangle\langle l_1|$ for $l_1 \neq l$, and the unity matrix $\hat{\mathbb{1}}$ describing the effective potential scattering.

We note that the effective interaction (63) can also be written in terms of reservoir field operators for a single reservoir only:

$$V_{\rm eff} = \sum_{kk'} :\tilde{\underline{a}}^{\dagger}_{k}\underline{\underline{\hat{J}}}\,\tilde{\underline{a}}_{k'}:, \tag{68}$$

where

$$\tilde{\underline{a}}_k = \sum_{\alpha}\underline{\underline{V}}^{\dagger}_{\alpha}\underline{a}_{\alpha k} \tag{69}$$

fulfill commutation relations of field operators for a single effective reservoir with N flavors due to the property (32). However, this is only possible if all the reservoirs can be taken together, i.e., they must have the same temperature and chemical potential. In nonequilibrium this is not possible. Nevertheless, for the poor man's scaling analysis described in the next section, this form of the Hamiltonian can be applied since the poor man's scaling analysis integrates out only energy

scales above the temperatures and chemical potentials of the reservoirs.

C. Poor man's scaling and fixed-point model for N levels

Taking the effective Hamiltonian in the cotunneling regime in the form (62) and (68), we now proceed to find an effective low-energy theory by integrating out all energy scales from the high-energy cutoff $\Lambda = D$ down to some low-energy scale Λ_c defined by the largest physical low-energy scale in the system set by the parameters $h_{ll'}$ of the dot Hamiltonian, the temperature T of the reservoirs, and the chemical potentials μ_α of the reservoirs

$$\Lambda_c = \max\{\{|h_{ll'}|\}_{ll'}, T, \{\mu_\alpha\}_\alpha\}. \tag{70}$$

This can be achieved by a standard poor man's scaling analysis leading to the RG equations

$$\frac{d\hat{J}_{ll'}}{ds} = -\sum_{l_1}\big[\hat{J}_{ll_1}, \hat{J}_{l_1l'}\big], \tag{71}$$

where $[\cdot,\cdot]$ denotes the commutator and $s = \ln\frac{D}{\Lambda}$ is the flow parameter. This RG equation has obviously the two invariants $\mathrm{Tr}\hat{J}_{ll'}$ and $\sum_l \hat{J}_{ll}$. Defining

$$\eta_l = \sum_{l'\neq l}\eta_{ll'}, \quad \eta = \sum_l \eta_l, \quad v = \sum_l v_l, \tag{72}$$

we obtain from the decomposition (65)

$$\mathrm{Tr}\hat{J}_{ll'} = N v_l \delta_{ll'}, \tag{73}$$

$$\langle l|\sum_{l'}\hat{J}_{l'l'}|l\rangle = \frac{1}{N}\eta - \eta_l + v, \tag{74}$$

and get the invariants

$$0 = \frac{d}{ds}v_l, \tag{75}$$

$$0 = \frac{d}{ds}\Big(\eta_l - \frac{1}{N}\eta\Big). \tag{76}$$

The first equation means that there is no renormalization for the potential scattering. The second equation holds for all $l = 1,\ldots,N$ and gives $N-1$ independent invariants.

Inserting the decomposition (65) in (71) we find after some straightforward algebra the RG equations for the parameters $\xi_{ll'}$ and $\eta_{ll'}$ characterizing the effective operator-valued matrix $\underline{\underline{\hat{J}}}$ at scale Λ in terms of (65) ($l \neq l'$ in all following equations):

$$\frac{d\xi_{ll'}}{ds} = 2\xi_{ll'}\bar{\eta}_{ll'} + \sum_{l_1\neq l,l'}\xi_{ll_1}\xi_{l_1l'}, \tag{77}$$

$$\frac{d\eta_{ll'}}{ds} = 2\xi_{ll'}\xi_{l'l} + \sum_{l_1\neq l,l'}\xi_{ll_1}\xi_{l_1l}, \tag{78}$$

where we defined the symmetric matrix

$$\bar{\eta}_{ll'} = \tfrac{1}{2}(\eta_{ll'} + \eta_{l'l}), \tag{79}$$

which fulfills the RG equation

$$\frac{d\bar{\eta}_{ll'}}{ds} = 2\xi_{ll'}^2 + \frac{1}{2}\sum_{l_1\neq l,l'}\big(\xi_{ll_1}^2 + \xi_{l_1l'}^2\big) \tag{80}$$

since $\xi_{ll'}$ stays symmetric during the whole RG flow

$$\xi_{ll'} = \xi_{l'l}. \tag{81}$$

These differential equations have to be solved starting from the initial conditions at $s = 0$ given by (66).

The RG equation for $\eta_{ll'}$ can be solved by the ansatz

$$\eta_{ll'} = \bar{\eta}_{ll'} + r_l - r_{l'}, \tag{82}$$

where the r_l are determined from the RG equations

$$\frac{dr_l}{ds} = \frac{1}{2}\sum_{l'\neq l}\xi_{ll'}^2, \tag{83}$$

with initial condition $r_l = \gamma_l^2/D$. Using the form (82) we can express the $N-1$ independent invariants (76) as

$$0 = \frac{d}{ds}\Big(r - Nr_l + \bar{\eta}_l - \frac{1}{N}\bar{\eta}\Big), \tag{84}$$

where we have defined in analogy to (72)

$$\bar{\eta}_l = \sum_{l'\neq l}\bar{\eta}_{ll'}, \quad \bar{\eta} = \eta = \sum_l \bar{\eta}_l, \quad r = \sum_l r_l. \tag{85}$$

With these invariants all $N-1$ differences $r_l - r_{l'}$ can be expressed via the symmetric matrix $\bar{\eta}_{ll'}$ and it is only necessary to consider the RG equations (77) and (80) for the symmetric matrices $\xi_{ll'}$ and $\bar{\eta}_{ll'}$. As we will see in Sec. II D, these coupling constants can be interpreted as the transverse and longitudinal Kondo couplings $J_\perp$ and J_z corresponding to the SU(2) subgroup formed by the level pair (l,l').

As one can see from (78), the parameters $\eta_{ll'}$ obtain a significant dependence on l' not present in the initial condition. Furthermore, all parameters $\xi_{ll'}$ and $\eta_{ll'}$ stay positive and increase monotonously under the RG flow until they diverge at a certain low-energy scale T_K. The fixed point is the one where all parameters are the same and proportional to an isotropic Kondo-type coupling J:

$$\xi_{ll'} = \eta_{ll'} = \tfrac{1}{2}J, \tag{86}$$

where J fulfills the RG equation (42):

$$\frac{dJ}{ds} = \frac{N}{2}J^2 \quad \Rightarrow \quad T_K = \Lambda e^{-\frac{2}{NJ}} = \text{const.} \tag{87}$$

T_K is the energy scale where all coupling constants diverge and is called the Kondo temperature in the following. This scale is exponentially sensitive to the choice of the initial conditions. Therefore, one defines a typical initial coupling J_0 via

$$\frac{4\gamma_l^2}{D} = y_l J_0, \quad \sum_l y_l = 1, \tag{88}$$

such that $y_l \sim O(1)$ are fixed parameters, and defines formally the scaling limit by

$$J_0 \to 0, \quad D \to \infty, \quad T_K = \text{const.} \tag{89}$$

Close to the fixed point we can neglect the small potential scattering term and get from (65) the form

$$\hat{J}_{ll'} = \frac{1}{2}J|l'\rangle\langle l|(1-\delta_{ll'}) + \frac{1}{2}J\sum_{l_1\neq l}\Big(\frac{1}{N}\hat{\mathbb{1}} - |l_1\rangle\langle l_1|\Big)\delta_{ll'}, \tag{90}$$

which can also be written in the more compact form

$$\hat{J}_{ll'} = \frac{1}{2} J |l'\rangle\langle l| - \frac{1}{2N} J \hat{\mathbb{1}} \delta_{ll'}. \tag{91}$$

Using this form in the effective interaction (68) we get at the fixed point in the one-particle subspace of the dot

$$V_{\rm eff} = -\frac{1}{2N} J \sum_{kk'} : \underline{\tilde{a}}_k^\dagger \underline{\tilde{a}}_{k'} : + \frac{1}{2} J \sum_{kk'} \sum_{ll'} c_{l'}^\dagger c_l \, : \tilde{a}_{lk}^\dagger \tilde{a}_{l'k'} : . \tag{92}$$

At the fixed point the effective interaction is obviously SU(N) invariant under a common unitary transformation of the N flavors of the reservoir and dot field operators. We note that this holds only in the case of the single reservoir described by the field operators $\tilde{a}_{lk}$ but not for the original model in nonequilibrium where the reservoirs have different chemical potentials μ_α. In this case one has to insert (69) in (92) and finds that the effective interaction is *not* invariant under a common unitary transformation of all dot field operators c_l and reservoir field operators $a_{\alpha lk}$ due to the presence of the matrices $\underline{\underline{V}}_\alpha$.

We finally show that the fixed-point Hamiltonian corresponds to a projection of the effective tunneling model (40) together with the potential scattering term (43) on the $N = 1$ subspace of the dot. Comparing (86) with (66), we find that we get indeed a unity matrix for $\underline{\underline{\gamma}} = \gamma \underline{\underline{\mathbb{1}}}$ with γ given by (41). Furthermore, the potential scattering is absent in the fixed-point model (90) and, therefore, we have to introduce the potential scattering term (43) in the effective tunneling model with a coupling constant $v_{\rm sc}$ given by (44) of opposite sign compared to (67) (where γ_l is replaced by γ) such that (43) cancels the potential scattering generated by projecting the effective tunneling model on the $N = 1$ subspace.

D. Poor man's scaling in SU(3) representation

For the three-level case $N = 3$, which is the main subject of this paper, it is quite instructive to write the Hamiltonian and the poor man's scaling equations also in the representation of the generators of the SU(3) group. This provides a nice physical picture as to how the reservoir and dot F spins are coupled and how the interaction can be interpreted in terms of the dot and reservoir quark flavors.

Since each matrix element $\hat{J}_{ll'}$ is an operator in the three-dimensional dot space we can decompose it in the F-spin components $\hat{F}_i = \frac{1}{2}\hat{\lambda}_i$ of the dot as

$$\hat{J}_{ll'} = \sum_{i=1}^{8} J_{ll'}^i \hat{F}_i + v_l \delta_{ll'} \hat{\mathbb{1}}, \tag{93}$$

where the last term contains the potential scattering. Furthermore, each 3×3 matrix $\underline{\underline{J}}^i$ can again be decomposed in the generators $\underline{\underline{\lambda}}_j$ in reservoir space [note that we still consider here only one effective reservoir due to the form (68) of the effective interaction in the poor man's scaling regime]. Comparing (93) with (65) we find after some straightforward algebra

$$\underline{\underline{J}}^i = J_i \underline{\underline{\lambda}}_i \quad \text{for } i = 1,2,4,5,6,7, \tag{94}$$

$$\underline{\underline{J}}^3 = J_3 \underline{\underline{\lambda}}_3 + J_{38} \underline{\underline{\lambda}}_8 + \frac{2}{3} c_3 \underline{\underline{\mathbb{1}}}, \tag{95}$$

$$\underline{\underline{J}}^8 = J_8 \underline{\underline{\lambda}}_8 + J_{83} \underline{\underline{\lambda}}_3 + \frac{2}{3\sqrt{3}} c_8 \underline{\underline{\mathbb{1}}}, \tag{96}$$

where the various coupling constants are defined by

$$J_1 = J_2 = \xi_{12}, \quad K_1 = \bar{\eta}_{12}, \tag{97}$$

$$J_4 = J_5 = \xi_{13}, \quad K_4 = \bar{\eta}_{13}, \tag{98}$$

$$J_6 = J_7 = \xi_{23}, \quad K_6 = \bar{\eta}_{23}, \tag{99}$$

$$J_3 = K_1, \quad J_8 = \frac{1}{3}(2K_4 + 2K_6 - K_1), \tag{100}$$

$$J_{38} = J_{83} = \frac{1}{\sqrt{3}}(K_4 - K_6), \tag{101}$$

together with the two invariants

$$c_3 = \frac{\gamma_1^2 - \gamma_2^2}{D}, \quad c_8 = \frac{\gamma_1^2 + \gamma_2^2 - 2\gamma_3^2}{D}. \tag{102}$$

c_3 and c_8 must be invariants since

$$\sum_l \hat{J}_{ll} = \sum_{i=1}^{8} (\mathrm{Tr}\underline{\underline{J}}^i)\, \hat{F}_i + v\hat{\mathbb{1}} \tag{103}$$

is an invariant such that all coefficients $\mathrm{Tr}\underline{\underline{J}}^i$ must be invariants for $i = 1, \ldots 8$. Using (94)–(96), we see that the trace for $i = 1,2,4,5,6,7$ is trivially zero but for $i = 3,8$ we get that $\mathrm{Tr}\underline{\underline{J}}^3 = 2c_3$ and $\mathrm{Tr}\underline{\underline{J}}^8 = (2/\sqrt{3})c_8$ must be invariants.

We note that only the six coupling constants $(J_1, J_4, J_6) = (\xi_{12}, \xi_{13}, \xi_{23})$ and $(K_1, K_4, K_6) = (\bar{\eta}_{12}, \bar{\eta}_{13}, \bar{\eta}_{23})$ are independent. This is consistent with our general analysis in Sec. II C where we showed that only the parameters $\xi_{ll'}$ and $\bar{\eta}_{ll'}$ are needed.

Since all coupling constants grow under the RG flow and diverge at T_K, the small invariants c_3, c_8, and v_l can be omitted from the effective interaction $V_{\rm eff}$ defined in (68). Inserting $\underline{\underline{\hat{J}}} \approx \sum_{i=1}^{8} \underline{\underline{J}}^i \hat{F}_i$ from (93) and the decompositions (94)–(96) we can write $V_{\rm eff}$ in the compact form

$$V_{\rm eff} = 2 \sum_{i=1}^{8} J_i \hat{f}_i \hat{F}_i + 2J_{38}(\hat{f}_8 \hat{F}_3 + \hat{f}_3 \hat{F}_8), \tag{104}$$

where we defined the reservoir f-spin operator as

$$\hat{f}_i = \frac{1}{2} \sum_{kk'} \underline{\tilde{a}}_k^\dagger \underline{\underline{\lambda}}_i \underline{\tilde{a}}_{k'}. \tag{105}$$

The form (104) exhibits very clearly how the reservoir f spin couples to the dot F spin. There are three possible isospin pairs formed by the up/down quark ($i = 1,2$), the up/strange quark ($i = 4,5$), or the down/strange quark ($i = 6,7$), corresponding to the flavor pairs $l = 1,2$, $l = 1,3$, and $l = 2,3$, respectively. For each isospin pair we can define a transverse and longitudinal coupling, denoted by (J_1, K_1), (J_4, K_4), and (J_6, K_6), respectively, analog to the transverse and longitudinal Kondo couplings $(J_\perp, J_z)$ for a single spin $\frac{1}{2}$. The three transverse couplings belong to the six independent generators λ_i for $i = 1,2,4,5,6,7$. Therefore, the effective interaction does not contain any transverse couplings between different isospins of the reservoir and the dot but only the product $\hat{f}_i \hat{F}_i$ for $i = 1,2,4,5,6,7$. In contrast, the three longitudinal parts of

the isospins are not independent. By convention, one chooses the longitudinal part of the up/down isospin (represented by λ_3) and the sum over the longitudinal parts of the up/strange and down/strange isospins (represented by the hypercharge generator $\sqrt{3}\lambda_8$) as basis for the two independent traceless matrices. Therefore, there is not only a longitudinal isospin coupling J_3 and a hypercharge coupling J_8 but also a mixed coupling J_{38} describing an interaction of the longitudinal reservoir isospin with the hypercharge polarization of the dot and vice versa. This picture naturally generalizes to arbitrary N providing a physical interpretation of the coupling constants ξ_{ij} and $\bar{\eta}_{ij}$ in terms of the transverse and longitudinal couplings for the isospin formed by the two flavors $l = i, j$.

Using (77) and (80) for $N = 3$, we obtain the RG equations

$$\frac{dJ_1}{ds} = 2J_1\,K_1 + J_4\,J_6, \tag{106}$$

$$\frac{dJ_4}{ds} = 2J_4\,K_4 + J_1\,J_6, \tag{107}$$

$$\frac{dJ_6}{ds} = 2J_6\,K_6 + J_1\,J_4, \tag{108}$$

$$\frac{dK_1}{ds} = 2J_1^2 + \frac{1}{2}\left(J_4^2 + J_6^2\right), \tag{109}$$

$$\frac{dK_4}{ds} = 2J_4^2 + \frac{1}{2}\left(J_1^2 + J_6^2\right), \tag{110}$$

$$\frac{dK_6}{ds} = 2J_6^2 + \frac{1}{2}\left(J_1^2 + J_4^2\right), \tag{111}$$

with the initial conditions at $s = 0$ given by (66):

$$J_1(0) = \frac{2\gamma_1\gamma_2}{D}, \quad J_4(0) = \frac{2\gamma_1\gamma_3}{D}, \tag{112}$$

$$J_6(0) = \frac{2\gamma_2\gamma_3}{D}, \quad K_1(0) = \frac{\gamma_1^2 + \gamma_2^2}{D}, \tag{113}$$

$$K_4(0) = \frac{\gamma_1^2 + \gamma_3^2}{D}, \quad K_6(0) = \frac{\gamma_2^2 + \gamma_3^2}{D}. \tag{114}$$

A numerical study of these RG equations shows that independent of the initial conditions, all couplings become equal during the RG flow and diverge at some low-energy scale T_K, in agreement with (86). Using (97)–(101), this means that all $J_i = J/2$ become the same for $i = 1, \ldots, 8$ and the mixed coupling J_{38} scales to zero. Thus, at the fixed point the effective interaction can be written in the isotropic and SU(3)-invariant form

$$V_{\text{eff}} = J \sum_{i=1}^{8} \hat{f}_i\,\hat{F}_i, \tag{115}$$

which is identical with (92). Applying the analog scheme to an arbitrary number N of dot levels we obtain at the fixed point the same result, one just has to sum in (115) over all generators of SU(N). Figure 2 shows an example for the RG flow where the longitudinal and transverse couplings $K_i \approx J_i$ are initially nearly the same but different for each $i = 1,4,6$.

To obtain a feeling for the nature of the strong-coupling ground state, we assume a two-site model with Hamiltonian (115). In particular, we consider a tight-binding model for the reservoir and the two sites are the dot and the first site of the reservoir (i.e., the one that couples to the dot), respectively,

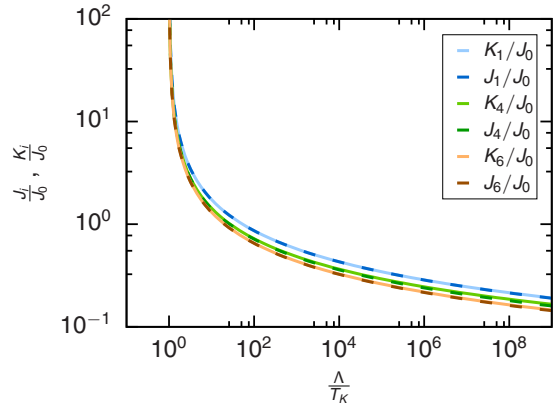

FIG. 2. Flow of the poor man's scaling RG for the couplings with similar initial values $(J_1, J_4, J_6)(0) = (0.018235, 0.015321, 0.013784)J_0$, $(K_1, K_4, K_6)(0) = (0.018337, 0.015924, 0.013994)J_0$, $J_0 = 0.096510$, and $D = 1000.0$. The couplings become degenerate at the Kondo scale T_K and diverge.

while the other reservoir sites are not taken into account. The crucial point about determining the ground state lies in choosing the appropriate representation for the eigenstates of the SU(3)-symmetric interaction in (115). The SU(3) group has two fundamental representations [38], which we denote by the multiplet notation [3] and $[\bar{3}]$. We represent the eigenstates of the dot in the representation [3] where the F-spin components are $\hat{F}_i = \frac{1}{2}\hat{\lambda}_i$. Denoting the states by the quark flavors $l = 1,2,3 = u,d,s$, we have

$$|u\rangle = \left|\tfrac{1}{2}, \tfrac{1}{3}\right\rangle, \tag{116}$$

$$|d\rangle = \left|-\tfrac{1}{2}, \tfrac{1}{3}\right\rangle, \tag{117}$$

$$|s\rangle = \left|0, -\tfrac{2}{3}\right\rangle, \tag{118}$$

where the states on the right-hand side are the eigenstates of $\hat{F}_3$ and $\hat{F}_8$ and the first (second) quantum number in the label is the corresponding eigenvalue of $\hat{F}_3$ ($\frac{2}{\sqrt{3}}\hat{F}_8$). Therefore, we refer to these eigenvalues as isospin (hypercharge) quantum numbers. Choosing the same representation for the first site in the reservoir is not useful since the states of the composite system are part of either the sextet [6] or the triplet $[\bar{3}]$ due to $[3] \otimes [3] = [6] \oplus [\bar{3}]$ [38]. Such a representation is not suitable since the system has a distinct nondegenerate ground state. Instead, we represent the first site of the reservoir with $[\bar{3}]$ and obtain $[3] \otimes [\bar{3}] = [8] \oplus [1]$ where all but one state of the two-site system form an octet together with the remaining state being a unique singlet state. $[\bar{3}]$ is the complex-conjugate representation of [3] and has therefore the generators $\hat{f}_i = -\frac{1}{2}\hat{\lambda}_i^*$. Consequently, we label the states of the second site with the antiquark flavor $\bar{l} = 1,2,3 = \bar{u},\bar{d},\bar{s}$ and get

$$|\bar{u}\rangle = \left|-\tfrac{1}{2}, -\tfrac{1}{3}\right\rangle, \tag{119}$$

$$\left|\bar{d}\right\rangle = \left|\tfrac{1}{2}, -\tfrac{1}{3}\right\rangle, \tag{120}$$

$$|\bar{s}\rangle = \left|0, \tfrac{2}{3}\right\rangle. \tag{121}$$

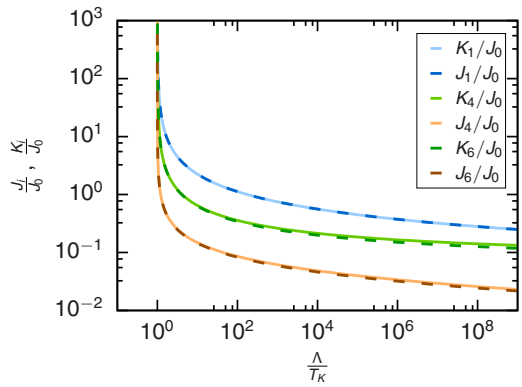

FIG. 3. Flow of the poor man's scaling RG for the couplings for $J_1(0) \gg J_4(0), J_6(0)$ with $(J_1, J_4, J_6)(0) = (0.0239873, 0.0022176, 0.0020878)J_0$, $(K_1, K_4, K_6)(0) = (0.0240310, 0.0128358, 0.0113882)J_0$, $J_0 = 0.0965099$, $D = 1000.0$. Each of the coupling pairs (J_1, K_1), (J_4, J_6), and (K_4, K_6) are quasidegenerate for the main part of the RG flow before all couplings obtain the same value at T_K.

In this basis, the operators $\hat{\lambda}_i^*$ have the same matrix representation as the Gell-Mann matrices $\hat{\lambda}_i$.

Indeed, we will show in Appendix B that the singlet state

$$|\mathrm{gs}\rangle = \frac{1}{\sqrt{3}}(|u\bar{u}\rangle + |d\bar{d}\rangle + |s\bar{s}\rangle) \tag{122}$$

is the ground state with energy $E_{\mathrm{gs}} = -\frac{4}{3}J$ while the octet states are degenerate with energy $E_8 = \frac{1}{6}J$. Since $|l\bar{l}\rangle = |l\rangle \otimes |\bar{l}\rangle$, it is straightforward to define the reduced dot density matrix

$$\hat{\rho} = \sum_{\bar{l}=\bar{u},\bar{d},\bar{s}} \langle\bar{l}|(|\mathrm{gs}\rangle\langle\mathrm{gs}|)|\bar{l}\rangle = \frac{1}{3}\hat{\mathbb{1}}, \tag{123}$$

which yields $n_l = \frac{1}{3}$ in perfect agreement with the NRG analysis in Sec. III.

Together with the SU(3)-symmetric interaction term, the outcome (122) motivates the term "quantum fluctuations" for the significant physical processes in the fixed-point model. The ground state is a symmetric linear combination of bound states with quark-antiquark flavor. This is in accordance with the observation that no free quarks exist, i.e., they always gather to form a particle with integer electric charge. The interaction term (115) preserves this since the fluctuation terms ($i = 1,2,4,5,6,7$) always annihilate a quark-antiquark pair while creating a different quark-antiquark bound state simultaneously. Furthermore, we will discuss in Appendix B that the eigenstates of (115) are identical to those of the quark model for light pseudoscalar mesons [39].

In this context, choosing $J_1 \approx K_1 \gg J_4 \approx J_6$ and $K_4 \approx K_6$ for the initial values reveals a nice physical picture in terms of the isospin of the up and down quarks. Figure 3 shows that in the whole regime from weak to intermediate coupling the couplings stay approximately degenerate with $J_1 \approx K_1$, $J_4 \approx J_6$, and $K_4 \approx K_6$. Here, the model exhibits an approximated SU(2) symmetry for the isospin with an isotropic isospin coupling $J_I = \frac{1}{2}(J_1 + K_1) \gg |J_1 - K_1|$. Furthermore, the interaction of isospin and hypercharge degrees of freedom disentangle in leading order since $J_{38} \ll J_3, J_8$. In the same way, $J_4 \approx J_6$ characterizes transitions between states differing in the hypercharge quantum number [compare with (116)–(118)]. In total, we find an isotropic isospin model where the presence of the third level (strange quark) mainly results in a potential scattering ($J_8 \sim J_I$) for the isospin with suppressed transitions to states with different hypercharge ($J_4, J_6 \ll J_I$). However, finally the RG flow approaches the generic SU(3)-symmetric fixed point on the Kondo scale T_K also in this case.

III. NRG ANALYSIS IN EQUILIBRIUM

In Sec. II D we have shown for a three-level quantum dot in the cotunneling regime that the generic fixed point model is an SU(3)-invariant isotropic effective interaction (115) between the F spins of the reservoir and the dot. This holds for the equilibrium case where all reservoirs can be taken together to a single reservoir and it requires also SU(3) symmetry of the dot. This means that the dot parameters $h_{ll'}$ have to be adjusted appropriately (including renormalizations arising from the coupling to the reservoir) such that the populations of all dot states are the same $n_l = \langle c_l^\dagger c_l\rangle = \frac{1}{3}$. The aim of this section is to confirm that in equilibrium the SU(3)-symmetric fixed point can be established independent of the tunneling matrix by an adjustment of the dot parameters. To this end, we use the numerically exact NRG method [40] and analyze the linear conductance G for $N = 3$ and two reservoirs ($\alpha = L, R$) for the case of proportional couplings $\underline{\underline{\Gamma}}_\alpha = x_\alpha \underline{\underline{\Gamma}}$ where G can be calculated from (18) and (16):

$$g = G/G_0 = -\frac{\pi}{2}\int d\omega\, \mathrm{Tr}\, \underline{\underline{\Gamma}}\, \underline{\underline{\rho}}(\omega)\, f'(\omega), \tag{124}$$

with the dimensionless conductance g in units of $G_0 = (e^2/h)/(4x_L x_R)$. As explained in Sec. II A the equilibrium spectral density $\underline{\underline{\rho}}(\omega)$ depends only on the total hybridization matrix $\underline{\underline{\Gamma}}$, i.e., we can use a unitary transformation of the dot states such that this matrix is diagonal [see (37)] and the spectral density in this basis depends only on the eigenvalues $\Gamma_l = 2\pi\gamma_l^2$. In this case, the linear conductance (124) can be written as

$$g = -\frac{\pi}{2}\int d\omega \sum_l \Gamma_l\, \rho_{ll}(\omega)\, f'(\omega). \tag{125}$$

In the new dot basis we assume for simplicity that the dot Hamiltonian contains only diagonal elements

$$H = \sum_l h_l c_l^\dagger c_l. \tag{126}$$

Other cases with nondiagonal elements $h_{ll'}$ can also be studied but are of no interest because they just destroy SU(3) symmetry of the dot and drive the system away from the fixed-point model. Here, we are interested in a systematic study how, for *arbitrary* tunneling parameters Γ_l, SU(3) symmetry can be restored by tuning the level positions h_l appropriately. In addition, we will also study the dependence of the SU(3) Kondo temperature $T_K^{(3)}$ as function of Γ_l and compare it to the corresponding SU(2) Kondo temperature $T_K^{(2)}$, where only two levels contribute to transport. This analysis goes beyond the one of Ref. [13] which has concentrated on the linear conductance

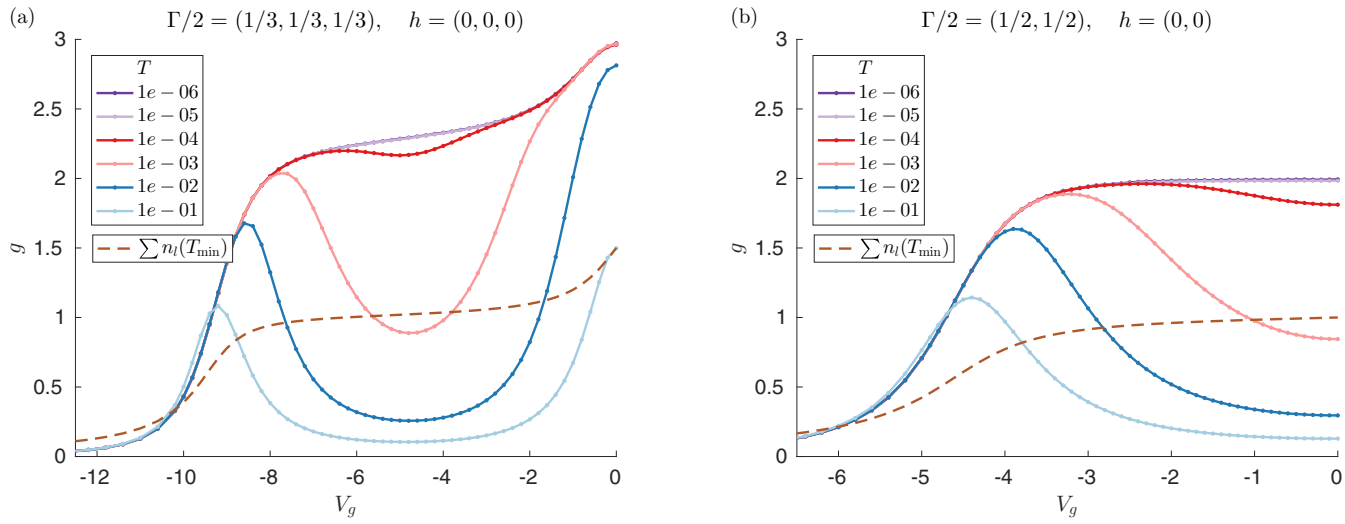

FIG. 4. Gate voltage dependence of the conductance at various temperatures for (a) $N = 3$ and (b) $N = 2$ at the SU(N)-symmetric point where all Γ_l are the same and all $h_l = 0$. By p-h symmetry the curves can be mirrored along $V_g = 0$. Also shown is the occupation n_l at the lowest temperature where the Friedel sum rule (127) is fulfilled.

for the SU(3)-symmetric case (i.e., all Γ_l are the same and $h_l = 0$) and the destruction of SU(3) symmetry by different Γ_l or finite values for $h_{ll'}$. As a signature of SU(3) symmetry we take the Friedel sum rule (used also in Refs. [12,13])

$$g = \sum_l \sin^2(\pi n_l), \tag{127}$$

which holds exactly at zero temperature and gives the value $g = 2.25$ for equal populations $n_l = \frac{1}{3}$ corresponding to the SU(3)-symmetric fixed point. The occupations n_l can be calculated from the spectral density via $n_l = \int d\omega\, \rho_{ll}(\omega) f(\omega)$. For the parameters in all figures we use

$$\frac{1}{2}\sum_l \Gamma_l = 1, \quad U = 10, \quad W = 10^4, \tag{128}$$

where $2W$ denotes the width of a flat DOS of the reservoirs [i.e., $|\omega| < W$ for the integral in (125)].

The calculations are performed using the full-density-matrix NRG [41], where we exploit either the individual charge conservation or the full SU(N) symmetry by means of the QSpace tensor library developed by Weichselbaum [42]. For the final results we employ a discretization parameter of $\Lambda = 3$, and we keep states up to a rescaled energy of $E_{\text{trunc}} = 9$ and maximal number N_{keep} during the NRG iteration. In the calculations without SU(N) symmetry we set $N_{\text{keep}} = 8000$. In the SU(N)-symmetric cases we can further increase the precision to very high level and explicitly confirm that results for g are converged up to 1% and results for n_l are converged up to 10^{-6} with respect to the numerical parameters. Note that in many calculations we optimize the level positions to achieve equal occupation of certain levels. Since the values of such optimized level positions h_l^* depend on the discretization of the bath, we refrain from using z averaging [40]. Finally, we need not broaden the NRG data as the computation of both g and n_l requires only discrete spectral weights.

To set the scene, we show in Fig. 4 known curves for the conductance depending on gate voltage and temperature in the SU(N)-symmetric cases for $N = 2,3$, where all Γ_l are the same and all $h_l = 0$. We find converged, plateaulike features when decreasing T below the Kondo temperature T_K in the cotunneling regime of a singly occupied dot. Note that n_l shows a very weak dependence on temperature in this regime and, at $T < T_K$, the Friedel sum rule (127) is fulfilled. Furthermore, we find that the Kondo temperatures $T_K^{(N)}$ are similar for $N = 2$ and 3 (recall that $\sum_l \Gamma_l$ is fixed). In contrast, the p-h symmetric point $V_g = 0$ corresponds to very different physics for the two cases since for $N = 3$ there are strong charge fluctuations due to $E_1 = E_2$, whereas for $N = 2$ spin fluctuations dominate. Therefore, at $V_g = 0$, the relevant low-energy scale is the hybridization Γ_l for $N = 3$ [13] and the Kondo temperature for $N = 2$.

Next, we study the case $\Gamma_1 = \Gamma_2 \neq \Gamma_3$ and $h_1 = h_2 = 0$. In this case, the different tunneling couplings lead to a different renormalization of h_3 of $O(\Gamma_1\Gamma_3/U)$ relative to $h_{1/2}$. Therefore, $h_1 = h_2 = h_3 = 0$ is *not* the SU(3)-symmetric point and the level position h_3 has to be adjusted appropriately to recover equal populations of the states and conductance $g = 2.25$ at zero temperature. Calling this optimized value h_3^* we show in Fig. 5 the conductance as function of $|h_3 - h_3^*|$. For temperatures $T < T_K^{(3)}$ we see that the conductance reaches the SU(3)-symmetric value $g = 2.25$ for $|h_3 - h_3^*| \sim T_K^{(3)}$ as expected. The Kondo temperature $T_K^{(3)}$ does not depend strongly on the value of Γ_3 and is nearly the same for $\Gamma_3 < \Gamma_{1/2}$ [Fig. 5(a)] and $\Gamma_3 > \Gamma_{1/2}$ [Fig. 5(b)]. For $|h_3 - h_3^*| > T_K^{(3)}$ and $h_3 > h_3^*$ (solid lines in Fig. 5), we see that the SU(2) Kondo effect with $g = 2$ appears at low enough temperatures $T < T_K^{(2)}$. Whereas $T_K^{(2)} \approx T_K^{(3)}$ for relatively small $\Gamma_3 < \Gamma_{1/2}$, we find that $T_K^{(2)} < T_K^{(3)}$ for $\Gamma_3 > \Gamma_{1/2}$. The latter can be explained by the fact that the two levels $l = 1,2$ form the SU(2) Kondo effect and therefore $T_K^{(2)}$ decreases if the coupling to these two levels Γ_1,Γ_2 is lowered. In contrast, when all three levels contribute to the SU(3) Kondo effect, we have a total coupling of $\sum_l \Gamma_l/2 = 1$ and find that the relative distribution of the Γ_l influences $T_K^{(3)}$ only weakly. Furthermore, in the regime where the SU(2) Kondo effect occurs, we see a strong

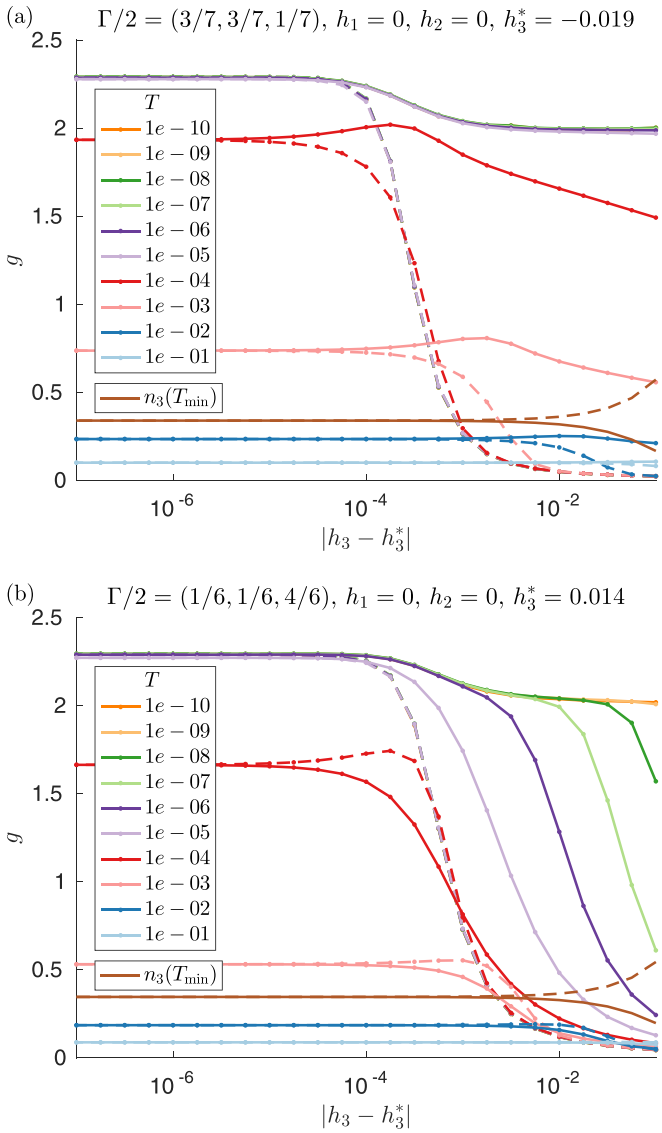

FIG. 5. Conductance at fixed $V_g = -U/2$ and $h_1 = h_2 = 0$ for (a) $\Gamma_1 = \Gamma_2 > \Gamma_3$ and (b) $\Gamma_1 = \Gamma_2 < \Gamma_3$ as function of $|h_3 - h_3^*|$ for various temperatures. We distinguish the case $h_3 > h_3^*$ (solid lines) from the case $h_3 < h_3^*$ (dashed lines), where h_3^* is the optimized value at which SU(3) symmetry is restored.

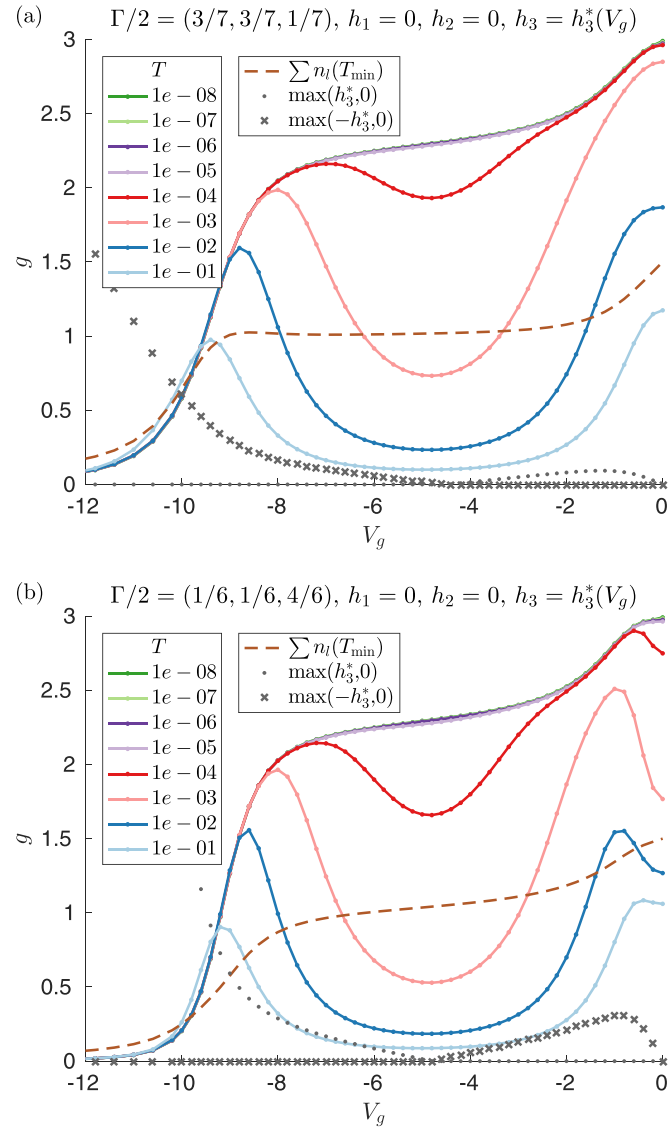

FIG. 6. Conductance for $h_1 = h_2 = 0$ and (a) $\Gamma_1 = \Gamma_2 > \Gamma_3$ and (b) $\Gamma_1 = \Gamma_2 < \Gamma_3$ as function of gate voltage for various temperatures. For each value of the gate voltage $h_3 = h_3^*(V_g)$ is optimized such that the populations of the three states are the same at zero temperature.

difference when moving over from $h_3 > h_3^*$ to $h_3 < h_3^*$ (dashed lines in Fig. 5) since then level 3 forms the ground state and thus the Kondo effect is much weaker compared to the case when the two levels $l = 1,2$ are lower in energy. In the regime of the SU(3) Kondo effect, it is hardly relevant whether level 3 approaches the other two levels from above or below.

In Fig. 6 we show the conductance as function of the gate voltage again for $h_1 = h_2 = 0$ and the two cases $\Gamma_1 = \Gamma_2 \gtrless \Gamma_3$ as in Fig. 5, but at each value of the gate voltage we choose the optimized value $h_3 = h_3^*(V_g)$ for which the populations of the three states are the same at zero temperature. As in Fig. 5 we confirm that $T_K^{(3)}$ depends only weakly on Γ_3 but the overall tendency is that $T_k^{(3)}$ decreases when increasing $|\Gamma_{1/2} - \Gamma_3|$. At the p-h symmetric point $V_g = 0$, the situation is completely different since charge fluctuations dominate for $N = 3$. Therefore, the conductance around $V_g = 0$ depends strongly on the relative distribution of the Γ_l. In fact, comparing various cases we find that the conductance at $V_g = 0$ (where also $h_3^* = 0$) decreases monotonously when increasing the variance of the couplings Γ_l. At large variance as in Fig. 6(b), g around $V_g = 0$ is strongly suppressed. In contrast, in the cotunneling regime $V_g \approx -U/2$ the conductance is rather insensitive to the distribution of the Γ_l. The combination of these phenomena leads to a surprising shape of the curve $g(V_g)$ which exhibits a local minimum at the p-h symmetric point for intermediate temperatures.

Finally, we consider in Fig. 7 three different hybridizations $\Gamma_1 < \Gamma_2 < \Gamma_3$ and tune h_2 and h_3 at fixed $h_1 = 0, V_g = -U/2$, and $T = 10^{-10}$. From the plots of the occupations n_l we can easily distinguish three regions where only one level is involved. At the intersections of two such regions we observe a two-level Kondo effect with conductance $g = 2$. The widths

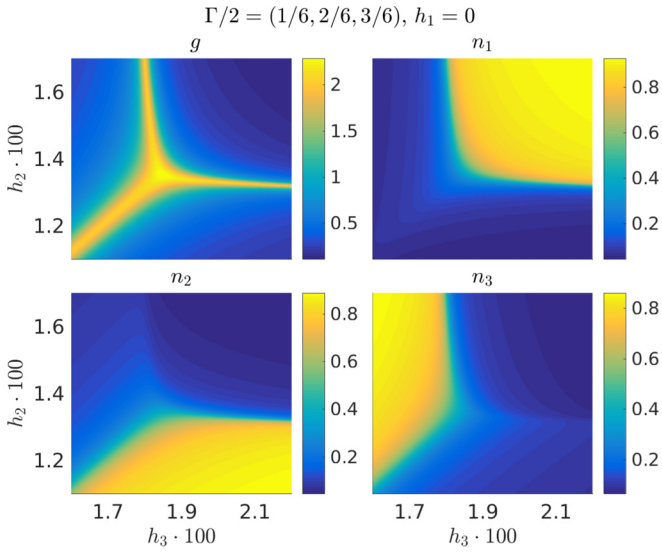

FIG. 7. Conductance and level occupations as functions of h_2 and h_3 for $\Gamma_1 < \Gamma_2 < \Gamma_3$, $h_1 = 0$, $V_g = -U/2$, and $T = 10^{-10}$.

of these intersections in the h_2-h_3 plane define three different Kondo temperatures $T_K^{(2)}$ which are ordered according to the size of the corresponding hybridizations $\Gamma_1 + \Gamma_2 < \Gamma_1 + \Gamma_3 < \Gamma_2 + \Gamma_3$. In the center, where all "one-level sections" intersect, we observe a wide region of a three-level Kondo effect with conductance $g = 2.25$. The corresponding Kondo temperature $T_K^{(3)}$ is of the same order as the maximum of the three two-level Kondo temperatures.

In summary, we find that for any kind of (diagonal) hybridization, whether with no, two, or three identical elements, we can find carefully optimized level positions (and low enough temperatures) to observe the behavior known from the SU(3)-symmetric quantum dot. For other hybridizations with two identical hybridization elements or, again, optimized level positions we can also reproduce the behavior of a two-level Kondo effect such that one level is (effectively) excluded. For arbitrary Γ_l and h_l (corresponding to most parts of a version of Fig. 7 zoomed out), the typical behavior is that of the single, (effectively) lowest-lying level.

IV. NONEQUILIBRIUM FIXED-POINT MODEL

The aim of this section is to analyze the *nonequilibrium* properties of the system for $N = 3$ in the perturbative regime where the cutoff scale Λ_c defined by (70) is much larger than the Kondo temperature $\Lambda_c \gg T_K$. Most importantly, as already emphasized several times in the previous sections, even if the fixed-point model (115) is reached at scale Λ_c [which will be the case if we take the formal scaling limit defined by (89)], it is essentially *not* SU(3) invariant if the chemical potentials of all reservoirs are different. This leads to new interesting nonequilibrium fixed-point models similar to the ones discussed in Ref. [21] for the $N = 2$ case which shows a completely different behavior of physical observables like the magnetization or the current compared to the SU(N)-symmetric Kondo model. Moreover, in practical situations the initial cutoff $D \sim E_c$ is fixed leading to deviations from the fixed-point model. Therefore, the aim of this section is to analyze the perturbative effects of the full effective interaction on physical observables and to identify a *smoking gun* for the fixed-point model together with a parameter measuring the distance from this fixed point.

A. Golden rule approach

We start from the effective interaction in the form (63) in terms of the original reservoir field operators $a_{\alpha lk}$. Inserting (93)–(96) and leaving out all small terms $\sim v_l, c_3, c_8$, we obtain

$$V_{\text{eff}} = \sum_{\alpha\alpha'} \sum_{kk'} : \underline{a}^\dagger_{\alpha k} \underline{\underline{V}}_\alpha \underline{\underline{\hat{J}}} \underline{\underline{V}}^\dagger_{\alpha'} \underline{a}_{\alpha' k'}, \tag{129}$$

with

$$\underline{\underline{\hat{J}}} \approx \sum_i \underline{\underline{J}}^i \hat{F}_i, \tag{130}$$

$$\underline{\underline{J}}^i = J_i \underline{\underline{\lambda}}_i + J_{38}(\delta_{i3} \underline{\underline{\lambda}}_8 + \delta_{i8} \underline{\underline{\lambda}}_3). \tag{131}$$

The total Hamiltonian is given by $H_{\text{tot}} = H_{\text{res}} + H_{\text{dot}} + V_{\text{eff}}$, with a unity DOS in the reservoirs and the dot Hamiltonian $H_{\text{dot}} = \sum_{ll'} h_{ll'} |l\rangle\langle l'|$ in the one-particle subspace. To apply the golden rule, we first diagonalize the dot Hamiltonian by a unitary transformation $\hat{U}$ such that

$$\tilde{H}_{\text{dot}} = \hat{U}^\dagger H_{\text{dot}} \hat{U} = \sum_l \epsilon_l |l\rangle\langle l|. \tag{132}$$

The golden rule rate for a transition from $l' \to l$ in the diagonalized basis is then given by

$$\Gamma_{l' \to l} = 2\pi \sum_{rr'} |\langle lr|\hat{U}^\dagger V_{\text{eff}} \hat{U}|l'r'\rangle|^2 \langle r'|\rho_{\text{res}}|r'\rangle \times \delta(\epsilon_l + E_r - \epsilon_{l'} - E_{r'}), \tag{133}$$

where $|r\rangle$ denote the many-particle states of the reservoirs with energy E_r and $\rho_{\text{res}} = \prod_\alpha \rho^\alpha_{\text{res}}$ is the product of the grand-canonical distributions of the reservoirs. Inserting the effective interaction (129) we find

$$\Gamma_{l' \to l} = 2\pi \sum_{\alpha\alpha'} \int d\omega \int d\omega' [1 - f_\alpha(\omega)] f_{\alpha'}(\omega') \times \delta(\epsilon_l - \epsilon_{l'} + \omega + \mu_\alpha - \omega' - \mu_{\alpha'}) \times \sum_{l_1 l_1'} |\langle l|\hat{U}^\dagger (\underline{\underline{V}}_\alpha \underline{\underline{\hat{J}}} \underline{\underline{V}}^\dagger_{\alpha'})_{l_1 l_1'} \hat{U}|l'\rangle|^2. \tag{134}$$

At zero temperature we get

$$\Gamma_{l' \to l} = 2\pi \sum_{\alpha\alpha'} w(\epsilon_l - \epsilon_{l'} + \mu_\alpha - \mu_{\alpha'}) \times \sum_{l_1 l_1'} |\langle l|\hat{U}^\dagger (\underline{\underline{V}}_\alpha \underline{\underline{\hat{J}}} \underline{\underline{V}}^\dagger_{\alpha'})_{l_1 l_1'} \hat{U}|l'\rangle|^2, \tag{135}$$

with $w(x) = |x|\theta(x)$. Here, $|\epsilon_l - \epsilon_{l'} + \mu_\alpha - \mu_{\alpha'}|$ is just the available energy phase space in the reservoirs for the energy gain $\epsilon_{l'} - \epsilon_l + \mu_{\alpha'} - \mu_\alpha > 0$. Inserting (130) we can write the

golden rate in the compact form

$$\Gamma_{l'\to l} = 2\pi \sum_{\alpha\alpha'} w(\epsilon_l - \epsilon_{l'} + \mu_\alpha - \mu_{\alpha'}) \times \sum_{ij} \langle l|\hat{U}^\dagger \hat{F}_i \hat{U}|l'\rangle \langle l'|\hat{U}^\dagger \hat{F}_j \hat{U}|l\rangle \, \tau_{ij}^{\alpha\alpha'}, \quad (136)$$

where

$$\tau_{ij}^{\alpha\alpha'} = \mathrm{Tr}\, \underline{\underline{V}}_\alpha^\dagger \underline{\underline{V}}_\alpha \underline{\underline{J}}^i \underline{\underline{V}}_{\alpha'}^\dagger \underline{\underline{V}}_{\alpha'} \underline{\underline{J}}^j. \quad (137)$$

As expected, only the combination $\underline{\underline{V}}_\alpha^\dagger \underline{\underline{V}}_\alpha$ enters into this expression which is consistent with our discussion in Sec. II A where it was shown that the hybridization matrices $\underline{\underline{\Gamma}}_\alpha$ depend only on this combination [see (36)].

The stationary probability distribution p_l in the diagonalized basis follows from

$$\sum_{l'} p_{l'}\, \Gamma_{l'\to l} = 0, \quad \sum_l p_l = 1. \quad (138)$$

In an analog way one can calculate the stationary current I_β flowing in reservoir β from the current rates $W_{ll'}^\beta$ in golden rule:

$$I_\beta = \sum_{ll'} p_{l'}\, \Gamma_{l'\to l}^\beta, \quad (139)$$

with

$$\sum_l \Gamma_{l'\to l}^\beta = 2\pi \sum_{\alpha\alpha'} (\delta_{\alpha\beta} - \delta_{\alpha'\beta}) w(\epsilon_l - \epsilon_{l'} + \mu_\alpha - \mu_{\alpha'}) \times \sum_{ij} \langle l|\hat{U}^\dagger \hat{F}_i \hat{U}|l'\rangle \langle l'|\hat{U}^\dagger \hat{F}_j \hat{U}|l\rangle \, \tau_{ij}^{\alpha\alpha'}. \quad (140)$$

Once the input of the matrices $\underline{\underline{V}}_\alpha$, the coupling constants (J_1, J_4, J_6) and (K_1, K_4, K_6) (determining the matrices $\underline{\underline{J}}^i$ for $i = 1, \ldots, 8$), the unitary transformation $\hat{U}$, and the eigenvalues ϵ_l of the dot Hamiltonian are known, the stationary probabilities and the current can be calculated in a straightforward way from the above golden rule expressions. Thereby, we have neglected small renormalizations of the dot parameters induced by the coupling to the reservoirs which are assumed to be much smaller than the level spacings in the dot.

B. *F*-spin magnetization for two reservoirs

We now calculate the F-spin magnetization of the dot

$$m_F = \sqrt{\sum_{i=1}^{8} (\langle \hat{F}_i \rangle)^2} \quad (141)$$

for the special case of two reservoirs. We will show that the condition of zero F-spin magnetization requires special dot parameters characterizing the deviation from the fixed-point model. In the basis of the diagonalized dot Hamiltonian, the density matrix of the dot is diagonal in the golden rule approximation so that only the two diagonal generators $\hat{F}_3$ and $\hat{F}_8$ contribute to m_F:

$$m_F = \sqrt{(\langle \hat{F}_3 \rangle)^2 + \langle \hat{F}_8 \rangle)^2} = \tfrac{1}{2}\sqrt{(p_1 - p_2)^2 + \tfrac{1}{3}(p_1 + p_2 - 2p_3)^2}. \quad (142)$$

Zero F-spin magnetization is then equivalent to an equal population of the three states

$$m_F = 0 \quad \Leftrightarrow \quad p_1 = p_2 = p_3. \quad (143)$$

As explained in Sec. II A via (49), the case of two reservoirs has the advantage that both matrices $\underline{\underline{V}}_\alpha^\dagger \underline{\underline{V}}_\alpha = \underline{\underline{U}}_V \underline{\underline{A}}_\alpha^{\mathrm{d}} \underline{\underline{U}}_V^\dagger$ can be diagonalized by a common unitary matrix $\underline{\underline{U}}_V$ and the diagonal matrices $\underline{\underline{A}}_\alpha^{\mathrm{d}}$ are parametrized via (51) by the parameters x_α, p_α, and q_α, which fulfill the conditions (52)–(54) and (28). Furthermore, it was shown that the special property of the fixed-point model is that the unitary transformation $\underline{\underline{U}}_V$ can be shifted to the dot such that in the new basis an effective diagonal tunneling model (56) emerges. Thus, the particular property of the fixed-point model is that the expectation value of the F-spin magnetization and the current I_α are independent of the unitary matrix $\underline{\underline{U}}_V$. In contrast, for the model away from the fixed point this is no longer the case.

The unitary matrix $\underline{\underline{U}}_V$ provides a mean to parametrize the dot Hamiltonian by convenient parameters. After transforming the dot Hamiltonian with $\hat{U}_V = \sum_{ll'} (\underline{\underline{U}}_V)_{ll'} |l\rangle\langle l'|$, we take the form

$$\hat{U}_V^\dagger H_{\mathrm{dot}} \hat{U}_V = h_x \hat{F}_1 + h_y \hat{F}_2 + h_z \hat{F}_3 + \frac{2}{\sqrt{3}} \Delta \hat{F}_8, \quad (144)$$

such that $\vec{h}$ can be interpreted as an effective magnetic field acting on the isospin of the up/down quark, and Δ is the level distance between the strange quark and the average level position of the up and down quarks:

$$\Delta = \tfrac{1}{2}(\epsilon_1 + \epsilon_2) - \epsilon_3 \quad (145)$$

(see also Fig. 1 for an illustration). The eigenvalues ϵ_l of H_{dot} and the unitary operator $\hat{U}$ can then be expressed by the dot parameters $\vec{h}$ and Δ by

$$\epsilon_{1/2} = \pm\frac{1}{2}h + \frac{1}{3}\Delta, \quad \epsilon_3 = -\frac{2}{3}\Delta, \quad (146)$$

$$\hat{U} = \hat{U}_V \hat{U}_h, \quad \underline{\underline{U}}_h = \left(\begin{array}{cc|c} \multicolumn{2}{c|}{\underline{x}_1\ \underline{x}_2} & 0 \\ \hline 0 & & 1 \end{array}\right), \quad (147)$$

where $h = \sqrt{h_\perp^2 + h_z^2}$, $h_\perp^2 = h_x^2 + h_y^2$, and

$$\underline{x}_{1/2} = \frac{1}{\sqrt{2h(h \mp h_z)}} \begin{pmatrix} \pm(h_x - i h_y) \\ h \mp h_z \end{pmatrix}. \quad (148)$$

Inserting $\hat{U} = \hat{U}_V \hat{U}_h$ and $\underline{\underline{V}}_\alpha^\dagger \underline{\underline{V}}_\alpha = \underline{\underline{U}}_V \underline{\underline{A}}_\alpha^{\mathrm{d}} \underline{\underline{U}}_V^\dagger$ in the golden rate (136) we get

$$\Gamma_{l'\to l} = 2\pi \sum_{\alpha\alpha'} w(\epsilon_l - \epsilon_{l'} + \mu_\alpha - \mu_{\alpha'}) \times \sum_{ij} \langle l|\hat{U}^\dagger \hat{U}_V^\dagger \hat{F}_i \hat{U}_V \hat{U}_h |l'\rangle \times \langle l'|\hat{U}_h^\dagger \hat{U}_V^\dagger \hat{F}_j \hat{U}_V \hat{U}_h |l\rangle \, \tau_{ij}^{\alpha\alpha'}, \quad (149)$$

with

$$\tau_{ij}^{\alpha\alpha'} = \mathrm{Tr}\, \underline{\underline{A}}^d_\alpha (\underline{\underline{U}}_V^\dagger \underline{\underline{J}}^i \underline{\underline{U}}_V) \underline{\underline{A}}^d_{\alpha'} (\underline{\underline{U}}_V^\dagger \underline{\underline{J}}^j \underline{\underline{U}}_V). \tag{150}$$

For the special case of the fixed-point model where $\underline{\underline{J}}^i = \frac{1}{2} J \underline{\underline{\lambda}}_i$, we can see that the unitary matrix $\underline{\underline{U}}_V$ indeed drops out as expected due to the invariant

$$\sum_{i=1}^{8} (\underline{\underline{U}}_V^\dagger \underline{\underline{\lambda}}_i \underline{\underline{U}}_V)(\hat{U}_V^\dagger \hat{F}_i \hat{U}_V) = \sum_{i=1}^{8} \underline{\underline{\lambda}}_i \hat{F}_i. \tag{151}$$

An analog property holds for the current rate (139).

In the following, we consider the strong nonequilibrium regime where the bias voltage $V = \mu_L - \mu_R > 0$ is assumed to be larger than all level spacings, i.e.,

$$V > |h|, |\Delta \pm h/2|. \tag{152}$$

From (142) we see directly that the condition $m_F = 0$ is equivalent to $\langle \hat{F}_3 \rangle = \langle \hat{F}_8 \rangle = 0$. Consequently, these are two conditions revealing that $m_F = m_F(h_z, h_\perp, \Delta) = 0$ generically defines a closed curve in $(h_z, h_\perp, \Delta)$ space. Inserting (51) for $\underline{\underline{A}}^d$, (131) for $\underline{\underline{J}}^i$, (146) for ϵ_l, and (147) for $\hat{U}_h$, we evaluate the golden rule rates (149) and (139) in Appendix C for the special case $\underline{\underline{U}}_V = \underline{\underline{\mathbb{1}}}$ from which we can determine the shape of this curve. This gives a generic result for the fixed-point model (where the matrix $\underline{\underline{U}}_V$ drops out), whereas for the model away from the fixed point we consider only the special case of a diagonal tunneling model.

From the condition $m_F(h_z, h_\perp, \Delta) = 0$ or $p_1 = p_2 = p_3 = 1/3$ we obtain in Appendix C the two equations

$$\Delta = x_L q_L V + \frac{J_4^2 - J_6^2}{J_4^2 + J_6^2} \left(x_L p_L V - \frac{1}{2} h_z \right), \tag{153}$$

$$\theta_2^2 x_L^2 p_L^2 V^2 = \theta_1^2 h_\perp^2 + \theta_2^2 (h_z - x_L p_L V)^2, \tag{154}$$

where

$$\theta_1^2 = J_1^2 + J_3^2 + J_{38}^2 + \tfrac{1}{2}(J_4^2 + J_6^2), \tag{155}$$

$$\theta_2^2 = 2J_1^2 + \tfrac{3}{2} J_4^2 - \tfrac{1}{2} J_6^2. \tag{156}$$

This means that the projection of the curve $m_F(h_z, h_\perp, \Delta) = 0$ on the $(h_z, h_\perp)$ plane is an ellipse with the ratio

$$s_1 = \theta_1 / \theta_2 \tag{157}$$

of the two shape parameters. θ_1 is the major axis (minor axis) if $s_1 > 1$ ($s_1 < 1$). We point out that this is different to the SU(2) model (i.e., $J_{38} = J_4 = J_6 = 0$) where θ_1 is always the major axis. Furthermore, the derivative of Δ with respect to h_z is given by

$$s_2 = \frac{d\Delta}{dh_z} = -\frac{1}{2} \frac{J_4^2 - J_6^2}{J_4^2 + J_6^2}. \tag{158}$$

The two parameters $s_{1/2}$ provide *smoking guns* for the detection of the fixed-point model since for $J_i = J/2$ and $J_{38} = 0$ we obtain

$$s_1 = 1, \quad s_2 = 0, \tag{159}$$

i.e., a circle in the $(h_z, h_\perp)$ plane as shown in Fig. 8 and no dependence of $\Delta = q_L V$ on h_z at the fixed point. In this sense

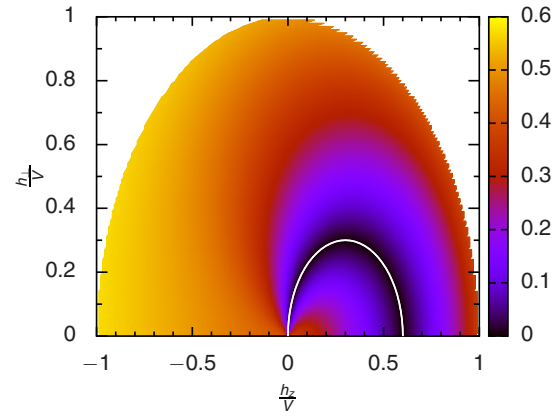

FIG. 8. The F-spin magnetization m_F in the strong nonequilibrium regime projected onto the $(h_z, h_\perp)$ plane at the fixed point with $x_L = x_R = 0.5$, $p_L = -p_R = 0.6$, $q_L = -q_R = 1.0$, $J = 0.0965103$, $V = 10^3\, T_K$, and $\Delta = 0.5V$. The white line $h_\perp^*(h_z)$ indicates where m_F is zero.

$1 - s_1$ and s_2 can both be viewed as parameters measuring the distance from the fixed-point model. Furthermore, we see that the parameters $x_L p_L = -x_R p_R$ and $x_L q_L = -x_R q_R$ of the fixed-point model can be determined from the two equations

$$\Delta = x_L q_L V, \quad h_\perp^2 + (h_z - x_L p_L V)^2 = x_L p_L^2 V^2. \tag{160}$$

To fix the remaining parameter $x_L x_R$ and the coupling J from a physical quantity we have also evaluated the current in Appendix C and obtained at the fixed point and for $m_F = 0$

$$\begin{aligned} I_L &= -I_R \\ &= \pi x_L x_R J^2 \left\{ -\frac{q_L - q_R}{6} \Delta - \frac{p_L - p_R}{4} h_z \right. \\ &\quad \left. + \frac{1}{3} \left(4 - \frac{q_L q_R}{9} - \frac{p_L p_R}{3} \right) V \right\} \\ &= \pi J^2 \left\{ \frac{1}{6} x_R q_R \Delta + \frac{1}{4} x_R p_R h_z \right. \\ &\quad \left. + \frac{1}{3} \left(4 x_L x_R + \frac{1}{9} x_R^2 q_R^2 + \frac{1}{3} x_R^2 p_L^2 \right) V \right\}, \end{aligned} \tag{161}$$

where we used $x_L x_R (q_L - q_R) = -x_R q_R$ and $x_L x_R (p_L - p_R) = -x_R p_R$ in the last equation. J^2 is just the overall scale of the current and the parameter $x_L x_R$ appears explicitly. Together with $x_L + x_R = 1$, the two parameters $x_{L/R}$ can thus be fixed.

In summary, we have shown in the strong nonequilibrium regime that the condition of vanishing F-spin magnetization $m_F = 0$ defines a closed curve in $(h_z, h_\perp, \Delta)$ space that is an ellipse in the special case of a diagonal tunneling model. A golden rule calculation has revealed that the geometric properties of this ellipse are a measure for the distance to the fixed-point model where the ellipse turns into a circle being embedded in a plane defined by a constant value for Δ. At the fixed point, the parameters of the effective model can experimentally be obtained from identifying the position of this circle together with measuring the current at the corresponding dot parameters $\vec{h}$ and Δ.

V. SUMMARY

The results obtained in this paper show that the area of nonequilibrium low-temperature transport through generic quantum dot models contains a huge variety of interesting fixed-point models not accessible in the equilibrium case. Previous studies have analyzed many generic Kondo scenarios for equilibrium systems and used the finite voltage V just as a probe for the equilibrium dot spectral density for quantum dots coupled very asymmetrically to two reservoirs [4]. In addition, the finite voltage together with corresponding decay rates was just expected to act as a cutoff scale for RG flows in the weak-coupling regime [23,24,27] analog to the temperature, leading to quantitatively but *not* qualitatively different physical properties. In contrast, the analysis performed in this paper shows that, for generic tunneling matrices, the cutoff set by the voltage is essentially different from the temperature since it drives the system towards a fixed point characterized by a *different symmetry* compared to the equilibrium case. Our main result is that if an electron on a singly occupied dot in the cotunneling regime can occupy N levels, flavor fluctuations lead to a model in the nonequilibrium situation which is essentially *not* SU(N) invariant. In the scaling limit for fixed values of V and T_K, a fixed-point model appears at scale V where each reservoir is characterized by N effective flavors with (N^2-1)-dimensional polarizations [corresponding to the N^2-1 generators of the SU(N) group] pointing in different directions such that the total sum is equal to zero. This leads to a SU(N)-symmetric equilibrium fixed point where all reservoirs can be taken together, but to a SU(N)-*nonsymmetric* nonequilibrium fixed point with *qualitatively* different physical properties. We have demonstrated this for the special case $N=3$ and two reservoirs in the weak-coupling regime $V \gg T_K$ and have seen that the condition of equal population of all dot states is realized for special dot parameters providing a *smoking gun* to identify the special symmetry of the nonequilibrium fixed-point model.

Strictly speaking, the numerical solution of the RG flow shows that even for rather large ratios D/T_K, the coupling constants become all equal only very close to T_K, where the poor man's scaling approach is no longer valid. This means that the fixed-point model can not be reached for voltages $V \gg T_K$, except for cases where the initial parameters have already been set close to the fixed point. It is therefore of high interest for the future to develop numerically exact approaches to describe the strong-coupling regime in nonequilibrium. In particular, for voltages $V \sim T_K$ we expect that the fixed-point model has been reached and the scaling of the conductance and the F-spin magnetization as function of the dot parameters will be essentially different from the SU(N)-symmetric case. In agreement with Refs. [12,13] we have demonstrated in this paper that in equilibrium the fixed-point model is indeed reached for temperatures below the Kondo temperature T_K, providing evidence that a similar result will also hold in the nonequilibrium case when the voltage reaches T_K. It will be interesting for the future to test this conjecture and to provide signatures of the nonequilibrium fixed-point model in the strong-coupling regime.

Finally, it will also be very interesting for the future to study the nonequilibrium fixed points in regimes where the particle number of the dot is larger than one $N_{\rm dot} > 1$. Already in the equilibrium case it has been demonstrated that not only the Coulomb interaction, but also other kinds of interactions (e.g., spin-dependent terms) are very important to find the correct ground state (see, e.g., Ref. [4] for a review). Based on this and our results for $N_{\rm dot} = 1$ we expect that even a richer variety of new nonequilibrium fixed-point models has to be expected for $N_{\rm dot} > 1$.

ACKNOWLEDGMENTS

This work was supported by the Deutsche Forschungsgemeinschaft via RTG 1995 (C.J.L. and H.S.). We thank A. Weichselbaum and S.-S. B. Lee for helpful discussions on the NRG setup. F.B.K. and J.v.D. acknowledge support by the Cluster of Excellence Nanosystems Initiative Munich; F.B.K. acknowledges funding from the research school IMPRS-QST.

APPENDIX A: RESERVOIR SELF-ENERGY

In this Appendix we calculate the greater/lesser self-energies $\underline{\underline{\Sigma}}^{\gtrless}_{\rm res}(\omega)$ of the dot arising from the tunneling Hamiltonian (7) with an effective tunneling matrix given by (40) together with the potential scattering term $V_{\rm sc}$ [see (43)]. The effective DOS of the reservoirs is given by unity since the whole nontrivial information of the reservoirs is included in the effective tunneling matrix. Using standard Keldysh formalism we get

$$\underline{\underline{\Sigma}}^{\gtrless}_{\rm res}(\omega) = \gamma^2 \sum_{\alpha\alpha'} \sum_{kk'} \underline{V}^{\dagger}_{\alpha} \, \underline{\underline{G}}^{\gtrless}_{\alpha k,\alpha' k'}(\omega) \, \underline{V}_{\alpha'}, \tag{A1}$$

where $\underline{\underline{G}}^{\gtrless}_{\alpha k,\alpha' k'}(\omega)$ are the greater/lesser reservoir Green's functions arising from the reservoir part of the Hamiltonian including the potential scattering term. These Green's functions can be calculated from the Dyson equation with $V_{\rm sc}$ defining the self-energy

$$\begin{aligned}\underline{\underline{G}}^{\gtrless}_{\alpha k,\alpha' k'}(\omega) = {} & \underline{\underline{g}}^{\gtrless}_{\alpha k}(\omega)\delta_{\alpha\alpha'}\delta_{kk'} \\ & + v_{\rm sc} \sum_{\alpha_1 k_1} \underline{\underline{g}}^{\gtrless}_{\alpha k}(\omega) \, \underline{V}_{\alpha} \, \underline{V}^{\dagger}_{\alpha_1} \, \underline{\underline{G}}^{A}_{\alpha_1 k_1,\alpha' k'}(\omega) \\ & + v_{\rm sc} \sum_{\alpha_1 k_1} \underline{\underline{g}}^{R}_{\alpha k}(\omega) \, \underline{V}_{\alpha} \, \underline{V}^{\dagger}_{\alpha_1} \, \underline{\underline{G}}^{\gtrless}_{\alpha_1 k_1,\alpha' k'}(\omega),\end{aligned} \tag{A2}$$

where $\underline{\underline{G}}^{A}_{\alpha_1 k_1,\alpha' k'}(\omega)$ denotes the advanced Green's function which follows from the Dyson equation

$$\begin{aligned}\underline{\underline{G}}^{A}_{\alpha k,\alpha' k'}(\omega) = {} & \underline{\underline{g}}^{A}_{\alpha k}(\omega)\delta_{\alpha\alpha'}\delta_{kk'} \\ & + v_{\rm sc} \sum_{\alpha_1 k_1} \underline{\underline{g}}^{A}_{\alpha k}(\omega) \, \underline{V}_{\alpha} \, \underline{V}^{\dagger}_{\alpha_1} \, \underline{\underline{G}}^{A}_{\alpha_1 k_1,\alpha' k'}(\omega).\end{aligned} \tag{A3}$$

$\underline{\underline{g}}^{x}_{\alpha k}$ (with $x = R, A, \gtrless$) denote the free Green's functions of reservoir α without $V_{\rm sc}$ given by

$$\underline{\underline{g}}^{R/A}_{\alpha k}(\omega) = \frac{1}{\omega - \epsilon_{\alpha k}\underline{\underline{\mathbb{1}}} \pm i\eta}, \tag{A4}$$

$$\underline{\underline{g}}^{<}_{\alpha k}(\omega) = -f_{\alpha}(\omega)(\underline{\underline{g}}^{R} - \underline{\underline{g}}^{A})(\omega), \tag{A5}$$

$$\underline{\underline{g}}^{>}_{\alpha k}(\omega) = [1 - f_{\alpha}(\omega)](\underline{\underline{g}}^{R} - \underline{\underline{g}}^{A})(\omega). \tag{A6}$$

Since the DOS of the reservoirs is unity we get

$$\sum_k \underline{\underline{g}}^{R/A}_{\alpha k}(\omega) = \mp i\pi \underline{\underline{\mathbb{1}}}, \tag{A7}$$

$$\sum_k \underline{\underline{g}}^{<}_{\alpha k}(\omega) = 2\pi i f_\alpha(\omega) \underline{\underline{\mathbb{1}}}, \tag{A8}$$

$$\sum_k \underline{\underline{g}}^{>}_{\alpha k}(\omega) = -2\pi i (1 - f_\alpha(\omega)) \underline{\underline{\mathbb{1}}}. \tag{A9}$$

Using these properties together with $\sum_\alpha \underline{\underline{V}}^\dagger_\alpha \underline{\underline{V}}_\alpha = \underline{\underline{\mathbb{1}}}$ and defining

$$\underline{\underline{\bar{G}}}^x(\omega) = \sum_{\alpha\alpha'} \sum_{kk'} \underline{\underline{V}}^\dagger_\alpha \underline{\underline{G}}^x_{\alpha k,\alpha' k'}(\omega) \underline{\underline{V}}_{\alpha'}, \tag{A10}$$

with $x = R, A, \gtrless$, we obtain from the Dyson equations (A2) and (A3) after a straightforward calculation

$$\underline{\underline{\bar{G}}}^A = i\pi \underline{\underline{\mathbb{1}}} + i\pi v_{\rm sc} \underline{\underline{\bar{G}}}^A, \tag{A11}$$

$$\underline{\underline{\bar{G}}}^<(\omega) = -i\pi v_{\rm sc} \underline{\underline{\bar{G}}}^<(\omega) + 2\pi i \sum_\alpha f_\alpha(\omega) \underline{\underline{V}}^\dagger_\alpha \underline{\underline{V}}_\alpha (\underline{\underline{\mathbb{1}}} + v_{\rm sc} \underline{\underline{\bar{G}}}^A), \tag{A12}$$

$$\underline{\underline{\bar{G}}}^>(\omega) = -i\pi v_{\rm sc} \underline{\underline{\bar{G}}}^>(\omega) - 2\pi i \sum_\alpha [1 - f_\alpha(\omega)] \underline{\underline{V}}^\dagger_\alpha \underline{\underline{V}}_\alpha (\underline{\underline{\mathbb{1}}} + v_{\rm sc} \underline{\underline{\bar{G}}}^A). \tag{A13}$$

Solving this set of matrix equations for $\underline{\underline{\bar{G}}}^{\gtrless}(\omega)$ and inserting the solution in

$$\underline{\underline{\Sigma}}^{\gtrless}_{\rm res}(\omega) = \gamma^2 \underline{\underline{\bar{G}}}^{\gtrless}(\omega), \tag{A14}$$

we finally get the result (11) and (12) for the self-energies with an effective hybridization matrix given by (47).

APPENDIX B: EQUILIBRIUM GROUND STATE OF THE FIXED-POINT MODEL

In Sec. II D, we have argued why the dot representation has the [3] fundamental representation while the first state of the reservoir the complex conjugate of this fundamental representation [$\bar{3}$]. Representing both sites by [3] (or, equivalently, by the complex conjugate of this representation [$\bar{3}$]) leads to a decomposition of the Hilbert space of the composite system into a sextet and a triplet. Accordingly, a SU(3)-symmetric Hamiltonian in this representation has an either threefold- or sixfold-degenerate ground state which is in contrast to the outcome of our analysis. Choosing the complex-conjugate representation [$\bar{3}$] for the reservoir site instead leads to a Hilbert space that decomposes into an octet and a singlet. A SU(3)-symmetric Hamiltonian in this representation yields two different eigenenergies of which one is nondegenerate and the other eightfold degenerate.

We want to emphasize that this is fundamentally different to the situation in the corresponding SU(2) model. Generally, the fundamental representation of the spin $\frac{1}{2}$ [2] is equivalent to its complex conjugate, i.e., [2] = [$\bar{2}$]. This is consistent with the observation that no antispin $\frac{1}{2}$ exists. However, this a special property of the SU(2) group that holds no longer for SU(N) with $N > 2$ and we anticipate for an analog SU(N) model a ground state inspired by flavor-antiflavor pairs.

We consider the following set of basis states for the composite system:

$$|u\bar{s}\rangle = |u\rangle \otimes |\bar{s}\rangle, \tag{B1}$$

$$|d\bar{s}\rangle = |d\rangle \otimes |\bar{s}\rangle, \tag{B2}$$

$$|d\bar{u}\rangle = |d\rangle \otimes |\bar{u}\rangle, \tag{B3}$$

$$|u\bar{d}\rangle = |u\rangle \otimes |\bar{d}\rangle, \tag{B4}$$

$$|s\bar{u}\rangle = |s\rangle \otimes |\bar{u}\rangle, \tag{B5}$$

$$|s\bar{d}\rangle = |s\rangle \otimes |\bar{d}\rangle, \tag{B6}$$

$$|u\bar{u}\rangle = |u\rangle \otimes |\bar{u}\rangle, \tag{B7}$$

$$|d\bar{d}\rangle = |d\rangle \otimes |\bar{d}\rangle, \tag{B8}$$

$$|s\bar{s}\rangle = |s\rangle \otimes |\bar{s}\rangle. \tag{B9}$$

In a quark picture, these states are meaningful since they are all eigenstates of the total charge operator

$$\hat{q}_{\rm tot} = \hat{Q} + \hat{q}, \tag{B10}$$

where $\hat{Q} = \hat{F}_3 + \frac{1}{\sqrt{3}}\hat{F}_8$ and $\hat{q} = \hat{f}_3 + \frac{1}{\sqrt{3}}\hat{f}_8$ are defined as usual in the quark model [38], with an integer eigenvalue. This is analog to the observation that no elementary particle with noninteger electrical charge exists in nature.

Let the effective Hamiltonian $V_{\rm eff}$ [Eq. (115)] act on the states (B1)–(B6), we find that $|u\bar{s}\rangle$, $|d\bar{s}\rangle$, $|d\bar{u}\rangle$, $|u\bar{d}\rangle$, $|s\bar{u}\rangle$, and $|s\bar{d}\rangle$ are eigenstates with eigenvalue $E_8 = \frac{1}{6}J$. Instead, the remaining states (B7)–(B9) are not eigenstates since

$$V_{\rm eff}|u\bar{u}\rangle = -\frac{J}{3}|u\bar{u}\rangle - \frac{J}{2}(|d\bar{d}\rangle + |s\bar{s}\rangle), \tag{B11}$$

$$V_{\rm eff}|d\bar{d}\rangle = -\frac{J}{3}|d\bar{d}\rangle - \frac{J}{2}(|u\bar{u}\rangle + |s\bar{s}\rangle), \tag{B12}$$

$$V_{\rm eff}|s\bar{s}\rangle = -\frac{J}{3}|s\bar{s}\rangle - \frac{J}{2}(|u\bar{u}\rangle + |d\bar{d}\rangle). \tag{B13}$$

Finding the remaining eigenstates is a trivial diagonalization problem in the 3×3 subspace of $|u\bar{u}\rangle$, $|d\bar{d}\rangle$, and $|s\bar{s}\rangle$. The first two linear combinations

$$|1\rangle = \frac{1}{\sqrt{2}}(|u\bar{u}\rangle - |d\bar{d}\rangle), \tag{B14}$$

$$|2\rangle = \frac{1}{\sqrt{6}}(|u\bar{u}\rangle + |d\bar{d}\rangle - 2|s\bar{s}\rangle) \tag{B15}$$

with eigenvalue E_8 complement the octet. Being orthogonal to $|1\rangle$ and $|2\rangle$, the singlet eigenstate is the ground state (122) with eigenvalue $E_{\rm gs} = -\frac{4}{3}J$. We note that this set of eigenstates is the same as for pseudoscalar mesons in the light quark model [39].

APPENDIX C: EVALUATION OF GOLDEN RULE RATE

In this Appendix we evaluate the golden rule rates (149) and (139) for the special case $\underline{\underline{U}}_V = \underline{\underline{\mathbb{1}}}$. We denote the three states by the quark flavors, i.e., $l = 1,2,3 \equiv u,d,s$. First, we evaluate the matrix elements $\tau_{ij}^{\alpha\alpha'}$ from (150) by employing the algebra of the Gell-Mann matrices. Writing

$$\tau_{ij}^{\alpha\alpha'} = x_\alpha x_{\alpha'} \bar{\tau}_{ij}^{\alpha\alpha'}, \tag{C1}$$

we obtain for the nonvanishing matrix elements

$$\bar{\tau}_{11}^{\alpha\alpha'} = \bar{\tau}_{22}^{\alpha\alpha'} = 2J_1^2 M_{1,\alpha\alpha'}^{-}, \tag{C2}$$

$$\bar{\tau}_{12}^{\alpha\alpha'} = -\bar{\tau}_{21}^{\alpha\alpha'} = 2iJ_1^2 M_{2,\alpha\alpha'}^{-}, \tag{C3}$$

$$\bar{\tau}_{44}^{\alpha\alpha'} = \bar{\tau}_{55}^{\alpha\alpha'} = J_4^2 M_{3,\alpha\alpha'}^{++}, \tag{C4}$$

$$\bar{\tau}_{45}^{\alpha\alpha'} = -\bar{\tau}_{54}^{\alpha\alpha'} = iJ_4^2 M_{3,\alpha\alpha'}^{+-}, \tag{C5}$$

$$\bar{\tau}_{66}^{\alpha\alpha'} = \bar{\tau}_{77}^{\alpha\alpha'} = J_6^2 M_{3,\alpha\alpha'}^{-+}, \tag{C6}$$

$$\bar{\tau}_{67}^{\alpha\alpha'} = -\bar{\tau}_{76}^{\alpha\alpha'} = iJ_6^2 M_{3,\alpha\alpha'}^{--}, \tag{C7}$$

$$\bar{\tau}_{ij}^{\alpha\alpha'}|_{i,j\in(3,8)} = 2J_{3i}J_{3j}M_{1,\alpha\alpha'}^{+} + 2J_{i8}J_{j8}M_{4,\alpha\alpha'} + \frac{2}{\sqrt{3}}(J_{3i}J_{j8} + J_{i8}J_{3j})M_{2,\alpha\alpha'}^{+}, \tag{C8}$$

where $J_{33} = J_3$, $J_{88} = J_8$, and

$$M_{1,\alpha\alpha'}^{\sigma} = \bar{q}_\alpha \bar{q}_{\alpha'} + \sigma p_\alpha p_{\alpha'}, \tag{C9}$$

$$M_{2,\alpha\alpha'}^{\sigma} = p_\alpha \bar{q}_{\alpha'} + \sigma \bar{q}_\alpha p_{\alpha'}, \tag{C10}$$

$$M_{3,\alpha\alpha'}^{\sigma\sigma'} = (\bar{q}_\alpha + \sigma p_\alpha)\tilde{q}_{\alpha'} + \sigma' \tilde{q}_\alpha (\bar{q}_{\alpha'} + \sigma p_{\alpha'}), \tag{C11}$$

$$M_{4,\alpha\alpha'} = 1 + \frac{p_\alpha p_{\alpha'} + q_\alpha q_{\alpha'}}{3} - \frac{q_\alpha + q_{\alpha'}}{3}, \tag{C12}$$

with $\bar{q}_\alpha = 1 + \frac{q_\alpha}{3}$ and $\tilde{q}_\alpha = 1 - \frac{2q_\alpha}{3}$. Introducing the notation

$$\chi_{1/3}^{\alpha\alpha'} = \frac{\pi}{2}\left(\tau_{11}^{\alpha\alpha'} \pm \tau_{33}^{\alpha\alpha'}\right), \tag{C13}$$

$$\chi_2^{\alpha\alpha'} = i\pi\tau_{12}^{\alpha\alpha'}, \quad \chi_s^{\alpha} = x_\alpha \tilde{q}_\alpha, \tag{C14}$$

$$\chi_{u/d}^{\alpha} = 2\pi x_\alpha [J_+^2(\bar{q}_\alpha \pm p_\alpha \phi_z) + J_-^2(p_\alpha \pm \bar{q}_\alpha \phi_z)], \tag{C15}$$

with $J_\pm^2 = \frac{1}{2}(J_4^2 \pm J_6^2)$ and $\phi_z = \frac{h_z}{h}$, we obtain by inserting (147) and (C1) in (149) after a straightforward calculation

$$\Gamma_{d\to u} = \sum_{\alpha\alpha'} w(\mu_\alpha - \mu_{\alpha'} - h) \times \left[\chi_1^{\alpha\alpha'} - \chi_2^{\alpha\alpha'}\phi_z + \chi_3^{\alpha\alpha'}\phi_z^2\right], \tag{C16}$$

$$\Gamma_{u\to d} = \sum_{\alpha\alpha'} w(\mu_\alpha - \mu_{\alpha'} + h)\left[\chi_1^{\alpha\alpha'} + \chi_2^{\alpha\alpha'}\phi_z + \chi_3^{\alpha\alpha'}\phi_z^2\right], \tag{C17}$$

$$\Gamma_{s\to u} = \sum_{\alpha\alpha'} w\left(\mu_\alpha - \mu_{\alpha'} - \Delta - \frac{h}{2}\right)\chi_u^\alpha \chi_s^{\alpha'}, \tag{C18}$$

$$\Gamma_{u\to s} = \sum_{\alpha\alpha'} w\left(\mu_\alpha - \mu_{\alpha'} + \Delta + \frac{h}{2}\right)\chi_s^\alpha \chi_u^{\alpha'}, \tag{C19}$$

$$\Gamma_{s\to d} = \sum_{\alpha\alpha'} w\left(\mu_\alpha - \mu_{\alpha'} - \Delta + \frac{h}{2}\right)\chi_d^\alpha \chi_s^{\alpha'}, \tag{C20}$$

$$\Gamma_{d\to s} = \sum_{\alpha\alpha'} w\left(\mu_\alpha - \mu_{\alpha'} + \Delta - \frac{h}{2}\right)\chi_s^\alpha \chi_d^{\alpha'}. \tag{C21}$$

In the following, we consider the case of two reservoirs in the strong nonequilibrium regime as defined in (152). From the properties (52)–(54) and the results (C1)–(C8) for $\tau_{ij}^{\alpha\alpha'}$, we obtain

$$\Gamma_{d\to u} = \left[\chi_1^{LR} - \chi_2^{LR}\phi_z + \chi_3^{LR}\phi_z^2\right](V - h) + w(-h)\sum_\alpha \left[\chi_1^{\alpha\alpha} + \chi_3^{\alpha\alpha}\phi_z^2\right], \tag{C22}$$

$$\Gamma_{u\to d} = \Gamma_{d\to u} + 2\chi_2^{LR}\phi_z V + h\left(\chi_1 + \chi_3\phi_z^2\right), \tag{C23}$$

$$\Gamma_{s\to u} = \chi_u^L \chi_s^R \left(V - \Delta - \frac{h}{2}\right) + w\left(-\Delta - \frac{h}{2}\right)\sum_\alpha \chi_u^\alpha \chi_s^\alpha, \tag{C24}$$

$$\Gamma_{u\to s} = \Gamma_{s\to u} + \left(\chi_s^L \chi_u^R - \chi_u^L \chi_s^R\right)V + \left(\Delta + \frac{h}{2}\right)\chi_u \chi_s, \tag{C25}$$

$$\Gamma_{s\to d} = \chi_d^L \chi_s^R \left(V - \Delta + \frac{h}{2}\right) + w\left(-\Delta + \frac{h}{2}\right)\sum_\alpha \chi_d^\alpha \chi_s^\alpha, \tag{C26}$$

$$\Gamma_{d\to s} = \Gamma_{s\to d} + \left(\chi_s^L \chi_d^R - \chi_d^L \chi_s^R\right)V + \left(\Delta - \frac{h}{2}\right)\chi_d \chi_s, \tag{C27}$$

where we have defined

$$\chi_{1/3} = \sum_{\alpha\alpha'} \chi_{1/3}^{\alpha\alpha'} = \pi\left[J_1^2 \pm J_3^2 \pm J_{38}^2\right], \tag{C28}$$

$$\chi_{u/d} = \sum_\alpha \chi_{u/d}^\alpha = 2\pi(J_+^2 \pm J_-^2\phi_z), \tag{C29}$$

$$\chi_s = \sum_\alpha \chi_s^\alpha = 1, \tag{C30}$$

and note that

$$\chi_2^{LR} = -2\pi J_1^2 x_L p_L, \tag{C31}$$

$$\chi_s^L \chi_{u/d}^R - \chi_{u/d}^L \chi_s^R = -2\pi[x_L q_L(J_+^2 \pm J_-^2\phi_z) + x_L p_L(J_-^2 \pm J_+^2\phi_z)]. \tag{C32}$$

The stationary probability distribution p_l follows from inserting (C22)–(C27) in (138). Finally, we can compute m_F from (142).

We note that $m_F = 0$ is equivalent to $\langle \hat{F}_3 \rangle = \langle \hat{F}_8 \rangle = 0$. Therefore, we consider $\langle \hat{F}_3 \rangle = \frac{1}{2}(p_u - p_d)$ and $\langle \hat{F}_8 \rangle = \frac{1}{3}(p_u + p_d - 2p_s)$ in the following and analyze under which conditions both expectation values become zero in the strong nonequilibrium regime. A cumbersome but straightforward

analysis yields

$$\langle \hat{F}_3 \rangle = \frac{1}{2N}[\mathcal{F}_1(\Gamma_{s\to u} + \Gamma_{s\to d}) + \mathcal{F}_2(\Gamma_{s\to u} - \Gamma_{s\to d})], \tag{C33}$$

$$\begin{aligned}\frac{2}{\sqrt{3}}\langle \hat{F}_8 \rangle = -\frac{1}{3N}\{&\mathcal{F}_1[2\pi J_+^2(h - 2x_L p_L \phi_z V) \\ &+ 4\pi J_-^2(\Delta - x_L q_L V)\phi_z + \Gamma_{s\to u} - \Gamma_{s\to d}] \\ &+ \mathcal{F}_2[2\mathcal{F}_2 + 2(\Gamma_{d\to u} + \Gamma_{u\to d}) + \Gamma_{s\to u} + \Gamma_{s\to d}]\}.\end{aligned} \tag{C34}$$

Here, the factor N follows from the normalization condition (138). Furthermore, we have defined the following functions in $(h_z, h_\perp, \Delta)$ space:

$$\begin{aligned}\mathcal{F}_1 = &-2\chi_2^{LR}\phi_z V - h\left(\chi_1 + \chi_3\phi_z^2\right) - \pi[J_+^2(h - 2x_L p_L \phi_z V) \\ &+ 2J_-^2(\Delta - x_L q_L V)\phi_z],\end{aligned} \tag{C35}$$

$$\mathcal{F}_2 = \pi[2J_+^2(\Delta - x_L q_L V) + J_-^2(h_z - 2p_l V)]. \tag{C36}$$

$\mathcal{F}_1 = \mathcal{F}_2 = 0$ fulfills the condition $\langle \hat{F}_3 \rangle = \langle \hat{F}_8 \rangle = 0$. Moreover, it defines a curve in $(h_z, h_\perp, \Delta)$ space that provides us with a tool to measure the distance to the fixed-point model. $\mathcal{F}_2 = 0$ directly yields (153) and defines the plane in $(h_z, h_\perp, \Delta)$ space where the curve lies in. The shape of the curve follows from $\mathcal{F}_1 = 0$. To that end, we insert (153) into (C35) and obtain (154). That is, we project the curve onto the $(h_z, h_\perp)$ plane.

Finally, we prove (161). To this end, we decompose (139) as

$$\begin{aligned}\langle I_\beta \rangle &= \sum_{ll'} \Gamma^\beta_{l'\to l} p_{l'} \\ &= I_0^\beta + I_3^\beta \langle \hat{F}_3 \rangle + I_8^\beta \frac{2}{\sqrt{3}}\langle \hat{F}_8 \rangle,\end{aligned} \tag{C37}$$

with

$$I_0^\beta = \frac{1}{3}\sum_{ll'} \Gamma^\beta_{l'\to l}, \tag{C38}$$

$$I_3^\beta = \sum_l \left(\Gamma^\beta_{u\to l} - \Gamma^\beta_{d\to l}\right), \tag{C39}$$

$$I_8^\beta = \frac{1}{2}\sum_l \left(\Gamma^\beta_{u\to l} + \Gamma^\beta_{d\to l} - 2\Gamma^\beta_{s\to l}\right). \tag{C40}$$

Evaluating (140) for two reservoirs in the strong nonequilibrium regime (152), we can express (C38)–(C40) in terms of $\bar{\tau}_{ij}^{\alpha\alpha'}$:

$$I_0^L = \frac{\pi}{3}x_L x_R\{\left[2\bar{\tau}_{11}^{LR} + \bar{\tau}_{33}^{LR} + 2\left(\bar{\tau}_{44}^{LR} + \bar{\tau}_{66}^{LR}\right) + \bar{\tau}_{88}^{LR}\right]V + 2i\left(\bar{\tau}_{45}^{LR} + \bar{\tau}_{67}^{LR}\right)\Delta + i\left(2\bar{\tau}_{12}^{LR} + \bar{\tau}_{45}^{LR} - \bar{\tau}_{67}^{LR}\right)h_z\}, \tag{C41}$$

$$\begin{aligned}I_3^L = \pi x_L x_R\Bigg\{&\left[2i\bar{\tau}_{12}^{LR} + \frac{2}{\sqrt{3}}\bar{\tau}_{38}^{LR} + \bar{\tau}_{44}^{LR} - \bar{\tau}_{66}^{LR} + i\left(\bar{\tau}_{45}^{LR} - \bar{\tau}_{67}^{LR}\right)\right]\phi_z V + \left[\bar{\tau}_{44}^{LR} - \bar{\tau}_{66}^{LR} + i\left(\bar{\tau}_{45}^{LR} - \bar{\tau}_{67}^{LR}\right)\right]\phi_z\Delta \\ &+ \left[\bar{\tau}_{11}^{LR} + \bar{\tau}_{33}^{LR} + \left(\bar{\tau}_{11}^{LR} - \bar{\tau}_{33}^{LR}\right)\phi_z^2 + \frac{1}{2}\left(\bar{\tau}_{44}^{LR} + \bar{\tau}_{66}^{LR}\right) + \frac{i}{2}\left(\bar{\tau}_{45}^{LR} + \bar{\tau}_{67}^{LR}\right)\right]h\Bigg\},\end{aligned} \tag{C42}$$

$$\begin{aligned}I_8^L = \frac{\pi}{2}x_L x_R\Bigg\{&\left[2\bar{\tau}_{11}^{LR} + \bar{\tau}_{33}^{LR} - \left(\bar{\tau}_{44}^{LR} + \bar{\tau}_{66}^{LR} + \bar{\tau}_{88}^{LR}\right) + 3i\left(\bar{\tau}_{45}^{LR} + \bar{\tau}_{67}^{LR}\right)\right]V + \left[3\left(\bar{\tau}_{44}^{LR} + \bar{\tau}_{66}^{LR}\right) - i\left(\bar{\tau}_{45}^{LR} + \bar{\tau}_{67}^{LR}\right)\right]\Delta \\ &+ \left[2i\bar{\tau}_{12}^{LR} + \frac{3}{2}\left(\bar{\tau}_{44}^{LR} - \bar{\tau}_{66}^{LR}\right) - \frac{i}{2}\left(\bar{\tau}_{45}^{LR} - \bar{\tau}_{67}^{LR}\right)\right]h_z\Bigg\}.\end{aligned} \tag{C43}$$

If we consider $m_F = 0$, the current I^β is completely equal to I_0^β. Therefore, we can evaluate (C42) using (C2)–(C8) at the fixed point and obtain (161).

[1] R. Hanson, L. P. Kouwenhoven, J. R. Petta, S. Tarucha, and L. M. K. Vandersypen, Rev. Mod. Phys. **79**, 1217 (2007).

[2] S. Andergassen, V. Meden, H. Schoeller, J. Splettstoesser, and M. R. Wegewijs, Nanotechnology **21**, 272001 (2010).

[3] A. C. Hewson, *The Kondo Problem to Heavy Fermions* (Cambridge University Press, Cambridge, 1997).

[4] L. I. Glazman and M. Pustilnik, in *Nanophysics: Coherence and Transport*, edited by H. Bouchiat *et al.* (Elsevier, Amsterdam, 2005), p. 427.

[5] L. I. Glazman and M. E. Raikh, Pis'ma Zh. Eksp. Teor. Fiz. **47**, 378 (1988) [Sov. Phys.–JETP Lett. **47**, 452 (1988)]; T. K. Ng and P. A. Lee, Phys. Rev. Lett. **61**, 1768 (1988).

[6] D. Goldhaber-Gordon, H. Shtrikman, D. Mahalu, D. Abusch-Magder, U. Meirav, and M. A. Kastner, Nature (London) **391**, 156 (1998); S. M. Cronenwett, T. H. Oosterkamp, and L. P. Kouwenhoven, Science **281**, 540 (1998); F. Simmel, R. H. Blick, J. P. Kotthaus, W. Wegscheider, and M. Bichler, Phys. Rev. Lett. **83**, 804 (1999).

[7] S. Sasaki, S. De Franceschi, J. M. Elzerman, W. G. van der Wiel, M. Eto, S. Tarucha, and L. P. Kouwenhoven, Nature (London) **405**, 764 (2000); J. Nygård, D. H. Cobden, and P. E. Lindelof, *ibid.* **408**, 342 (2000); J. Schmid, J. Weis, K. Eberl, and K. v. Klitzing, Phys. Rev. Lett. **84**, 5824 (2000); M. Eto and Yu. V. Nazarov, *ibid.* **85**, 1306 (2000); M. Pustilnik and L. I. Glazman, *ibid.* **85**, 2993 (2000).

[8] W. G. van der Wiel, S. De Franceschi, J. M. Elzerman, S. Tarucha, L. P. Kouwenhoven, J. Motohisa, F. Nakajima, and T. Fukui, Phys. Rev. Lett. **88**, 126803 (2002); M. Pustilnik and L. I. Glazman, *ibid.* **87**, 216601 (2001); W. Hofstetter and H. Schoeller, *ibid.* **88**, 016803 (2001); A. Kogan, G. Granger, M. A.

Kastner, D. Goldhaber-Gordon, and H. Shtrikman, Phys. Rev. B **67**, 113309 (2003); W. Hofstetter and G. Zaránd, *ibid.* **69**, 235301 (2004).

[9] Y. Oreg and D. Goldhaber-Gordon, Phys. Rev. Lett. **90**, 136602 (2003); R. M. Potok, I. G. Rau, H. Shtrikman, Y. Oreg, and D. Goldhaber-Gordon, Nature (London) **446**, 167 (2007); A. J. Keller, L. Peeters, C. P. Moca, I. Weymann, D. Mahalu, V. Umansky, G. Zaránd, and D. Goldhaber-Gordon, *ibid.* **526**, 237 (2015).

[10] L. Borda, G. Zaránd, W. Hofstetter, B. I. Halperin, and J. von Delft, Phys. Rev. Lett. **90**, 026602 (2003); S. Sasaki, S. Amaha, N. Asakawa, M. Eto, and S. Tarucha, *ibid.* **93**, 017205 (2004); P. Jarillo-Herrero, J. Kong, H. S. J. van der Zant, C. Dekker, and L. Kouwenhoven, Nature (London) **434**, 484 (2005); R. López, D. Sanchez, M. Lee, M. S. Choi, P. Simon, and K. Le Hur, Phys. Rev. B **71**, 115312 (2005); M. S. Choi, R. López, and R. Aguado, Phys. Rev. Lett. **95**, 067204 (2005); S. Amasha, A. J. Keller, I. G. Rau, A. Carmi, J. A. Katine, H. Shtrikman, Y. Oreg, D. and Goldhaber-Gordon, *ibid.* **110**, 046604 (2013).

[11] A. Carmi, Y. Oreg, and M. Berkooz, Phys. Rev. Lett. **106**, 106401 (2011); C. Moca, A. Roman, M. Toderaş, and R. Chirla, AIP Conf. Proc. **1916**, 030003 (2017).

[12] C. P. Moca, A. Alex, J. von Delft, and G. Zaránd, Phys. Rev. B **86**, 195128 (2012).

[13] R. López, T. Rejec, J. Martinek, and R. Žitko, Phys. Rev. B **87**, 035135 (2013).

[14] J. König and J. Martinek, Phys. Rev. Lett. **90**, 166602 (2003); M. Braun, J. König, and J. Martinek, Phys. Rev. B **70**, 195345 (2004); I. Weymann and J. Barnas, *ibid.* **75**, 155308 (2007).

[15] D. Boese, W. Hofstetter, and H. Schoeller, Phys. Rev. B **64**, 125309 (2001); **66**, 125315 (2002).

[16] V. Kashcheyevs, A. Schiller, A. Aharony, and O. Entin-Wohlman, Phys. Rev. B **75**, 115313 (2007).

[17] J. Paaske, A. Andersen, and K. Flensberg, Phys. Rev. B **82**, 081309(R) (2010).

[18] M. Pletyukhov and D. Schuricht, Phys. Rev. B **84**, 041309 (2011).

[19] J. Martinek, Y. Utsumi, H. Imamura, J. Barnas, S. Maekawa, J. König, and G. Schön, Phys. Rev. Lett. **91**, 127203 (2003); J. Martinek, M. Sindel, L. Borda, J. Barnas, J. König, G. Schön, and J. von Delft, *ibid.* **91**, 247202 (2003); M. Sindel, L. Borda, J. Martinek, R. Bulla, J. König, G. Schön, S. Maekawa, and J. von Delft, Phys. Rev. B **76**, 045321 (2007).

[20] Y. Meir and N. S. Wingreen, Phys. Rev. Lett. **68**, 2512 (1992).

[21] S. Göttel, F. Reininghaus, and H. Schoeller, Phys. Rev. B **92**, 041103(R) (2015).

[22] T. A. Costi, A. C. Hewson, and V. Zlatic, J. Phys.: Condens. Matter **6**, 2519 (1994).

[23] A. Rosch, J. Kroha, and P. Wölfle, Phys. Rev. Lett. **87**, 156802 (2001); A. Rosch, J. Paaske, J. Kroha, and P. Wölfle, *ibid.* **90**, 076804 (2003).

[24] S. Kehrein, Phys. Rev. Lett. **95**, 056602 (2005); P. Fritsch and S. Kehrein, Phys. Rev. B **81**, 035113 (2010).

[25] H. Schoeller, Eur. Phys. J. Special Topics **168**, 179 (2009); Dynamics of open quantum systems, in *Lecture Notes of the 45th IFF Spring School Computing Solids: Models, Ab initio Methods and Supercomputing* (Forschungszentrum Jülich, 2014).

[26] S. G. Jakobs, M. Pletyukhov, and H. Schoeller, Phys. Rev. B **81**, 195109 (2010); J. Eckel *et al.*, New J. Phys. **12**, 043042 (2010).

[27] H. Schoeller and F. Reininghaus, Phys. Rev. B **80**, 045117 (2009); **80**, 209901(E) (2009).

[28] M. Pletyukhov, D. Schuricht, and H. Schoeller, Phys. Rev. Lett. **104**, 106801 (2010).

[29] M. Pletyukhov and H. Schoeller, Phys. Rev. Lett. **108**, 260601 (2012); F. Reininghaus, M. Pletyukhov, and H. Schoeller, Phys. Rev. B **90**, 085121 (2014).

[30] S. Smirnov and M. Grifoni, Phys. Rev. B **87**, 121302(R) (2013); New J. Phys. **15**, 073047 (2013).

[31] A. V. Kretinin, H. Shtrikman, and D. Mahalu, Phys. Rev. B **85**, 201301(R) (2012); O. Klochan, A. P. Micolich, A. R. Hamilton, D. Reuter, A. D. Wieck, F. Reininghaus, M. Pletyukhov, and H. Schoeller, *ibid.* **87**, 201104(R) (2013).

[32] F. B. Anders and A. Schiller, Phys. Rev. Lett. **95**, 196801 (2005); F. B. Anders, R. Bulla, and M. Vojta, *ibid.* **98**, 210402 (2007); A. Hackl, D. Roosen, S. Kehrein, and W. Hofstetter, *ibid.* **102**, 219902(E) (2009).

[33] A. J. Daley, C. Kollath, U. Schollwoeck, and G. Vidal, J. Stat. Mech.: Theory Exp. (2004) P04005; S. R. White and A. E. Feiguin, Phys. Rev. Lett. **93**, 076401 (2004); P. Schmitteckert, Phys. Rev. B **70**, 121302 (2004); F. Heidrich-Meisner, A. E. Feiguin, and E. Dagotto, *ibid.* **79**, 235336 (2009).

[34] S. Weiss, J. Eckel, M. Thorwart, and R. Egger, Phys. Rev. B **77**, 195316 (2008).

[35] T. L. Schmidt, P. Werner, L. Mühlbacher, and A. Komnik, Phys. Rev. B **78**, 235110 (2008).

[36] F. Schwarz, I. Weymann, J. von Delft, and A. Weichselbaum, arXiv:1708.06315.

[37] C. Caroli, R. Combescot, P. Nozières, and D. Saint-James, J. Phys. C: Solid State Phys. **4**, 916 (1971); **5**, 21 (1972).

[38] S. Coleman, *Aspects of Symmetry*, 1st ed. (Cambridge University Press, Cambridge, 1985); H. Georgi, *Lie Algebras in Particle Physics: From Isospin to Unified Theories*, 2nd ed., Frontiers in Physics, Vol. 54 (Westview, Boulder, CO, 1999).

[39] D. Griffiths, *Introduction to Elementary Particles*, 2nd ed. (Wiley, Weinheim, 2008).

[40] R. Bulla, T. A. Costi, and T. Pruschke, Rev. Mod. Phys. **80**, 395 (2008).

[41] A. Weichselbaum and J. von Delft, Phys. Rev. Lett. **99**, 076402 (2007); A. Weichselbaum, Phys. Rev. B **86**, 245124 (2012).

[42] A. Weichselbaum, Ann. Phys. **327**, 2972 (2012).